



**Politecnico  
di Torino**

# **POLITECNICO DI TORINO**

**Master's Degree in Mechatronic Engineering**

**Master's Degree Thesis**

## **Study for the development of an electromechanical shifting system in a model-based approach**

**Academic Year 2020/2021**

**Supervisors**

**Prof. Andrea TONOLI**

**Prof. Nicola AMATI**

**Prof. Mario SILVAGNI**

**Company tutor**

**Edoardo MONGARLI**

**Candidate**

**Federica GUALA**

**October 2021**



## Abstract

The model based design is a design approach that is widely spreading in the technical environment. The center of this development process is the creation of a virtual model of the system of interest that is then used to perform design and test activities such as validation, optimisation and simulation on the designed object. It can also be used for automatic code generation or reporting, allowing companies to save money and time in the design phase and hence to be present early on the market scene. This project was developed in team with an electronic student colleague, in a company that produces gear shifting systems. The shifting system is a component used in the automotive industry to convert the driver's will into an action on the vehicle. This is realised by moving a mechanical cable that operates on the vehicle gearbox. The aim of this thesis is to exploit and adapt the model based approach in the development of an electromechanical automatic shifter system in order to create in the future an industrial component. The starting point was an already existing mechanical prototype of the system and its functioning requirements. First step was the studying phase with the aim to better understand the mechanical system already implemented, its working conditions and the expected results. Once the system behaviour was understood, a first model of the actuator using the Simulink - Matlab environment was built, at this stage of the work only in continuous time. The hardware components needed to supply the electrical motor in the actuator and the sensors to take data were identified, purchased by the company and the needed code for them to run was implemented. As soon as the hardware part was working, the first few tests on the DC motor were run in order to validate the parameters of the DC motor datasheet provided by the electrical motor manufacturers. The Simulink model was improved and converted in discrete time in order to exploit it for the design of the PWM used to regulate the voltage supplied by the H bridge component to the electrical DC motor. In order to model the remaining parts of the actuator, using a current sensor, different tests were performed to estimate the static and dynamic friction present in the actuator. Once the model has reached a satisfying accuracy, it was also exploited for the design of a suitable closed – loop control system. The chosen

control technique was the PID controller and the controlled variable the position of the mechanical cable to be moved. At last also the external loads opposing the movement of the mechanical cable were modeled. The completed model was used to tune the PID controller. Finally, after performing multiple simulations in the different working conditions, practical tests on the implemented actuator were performed.



# Table of Contents

<b>1</b>	<b>Introduction</b>	<b>1</b>
1.1	Sila Group . . . . .	2
1.2	Shifting systems . . . . .	3
<b>2</b>	<b>Mechanical prototype and functional requirements</b>	<b>4</b>
2.1	Mechanical prototype . . . . .	6
2.1.1	Electrical motor . . . . .	8
2.1.2	Transmission and runners . . . . .	8
2.1.3	Retaining system . . . . .	10
2.2	Functional requirements . . . . .	11
2.2.1	Normal operating mode . . . . .	11
2.2.2	Emergency mode . . . . .	13
<b>3</b>	<b>Model based design approach</b>	<b>14</b>
3.1	DC Motor model definition . . . . .	16
3.1.1	Electrical motor block scheme . . . . .	19
3.2	Transmission block scheme . . . . .	24
3.3	Loads block scheme . . . . .	26
3.3.1	Static and dynamic friction modelling . . . . .	27
3.3.2	Spring load modelling . . . . .	31
3.3.3	External gearbox load modelling . . . . .	33
3.4	Complete plant model . . . . .	40
<b>4</b>	<b>Hardware implementation</b>	<b>42</b>
4.1	Microcontroller . . . . .	43

4.2	Sensors . . . . .	45
4.2.1	Position sensor . . . . .	45
4.2.2	Current sensor . . . . .	48
4.3	Motor driver . . . . .	49
4.3.1	Pulse Width Modulation . . . . .	49
4.3.2	PWM modelling . . . . .	52
4.3.3	H bridge component . . . . .	53
<b>5</b>	<b>Model validation</b>	<b>55</b>
5.1	DC motor validation . . . . .	56
5.2	Transmission and spring validation . . . . .	60
5.3	Static and dynamic friction validation . . . . .	60
<b>6</b>	<b>Control design</b>	<b>62</b>
6.1	Closed loop control system . . . . .	63
6.2	PID control strategy . . . . .	65
6.3	PI modelling . . . . .	67
6.4	PI tuning . . . . .	69
<b>7</b>	<b>Testing</b>	<b>71</b>
7.1	No load condition test . . . . .	72
7.2	Spring loading test . . . . .	75
7.3	Disengaging P mode test . . . . .	78
<b>8</b>	<b>Conclusions</b>	<b>80</b>
	<b>Bibliography</b>	<b>82</b>



# Chapter 1

## Introduction

This master thesis is developed in collaboration with the R&D department of the company Sila Group. The aim of this work is the customer-specific handling of an electromechanical automatic shifting system.

The project started from the customer's specifications and ended with a working prototype. It is the result of the collaboration of three master thesis students from different branches of engineering: myself as a master thesis student in mechatronic engineering, a colleague master thesis student in electronic engineering with whom I work on the movement of the actuator, and a colleague master thesis student in automotive engineering who took care of the mechanical part of the prototype.

Our contribution to the project, of my electronic colleague and I, started from the purely mechanical prototype of the actuator and consisted in creating the correct movement of the components in the actuator in order to satisfy the functionalities required by the customer.

To achieve our goal, my colleague and I decided to implement a model based design approach, in order to study the already existing prototype and implement the hardware and software part needed to move the actuator according to the customer requirements. I personally took care of the modelling and control part of the work, while my colleague was responsible for choosing the needed hardware components and writing the firmware required for the electronic part to function. We worked in team resulting in sharing ideas and doubts, looking for the best solutions to solve the problems that have arisen during the development and testing

phase.

In order to achieve the goal, the project was divided into several work phases:

- Study of customer specifications and the mechanical part of the actuator
- Study of the functioning of a DC electrical motor and how to drive it
- Simulink model implementation and control strategy design
- Hardware and Firmware implementation
- Testing

The objectives of this thesis are therefore to study the system in order to derive a Simulink model to simulate its dynamics and to study a control strategy for the electrical motor, inside the actuator, suitable for implementing the required functionalities.

All this is aimed to achieving in the future an industrial component.

## **1.1 Sila Group**

Sila Holding Industriale SpA is a company founded in 1943 by Edoardo Brero. SILA, Società Italiana per la Lavorazione Acciai, originally was a producer of high pressure hydraulic pipelines.

In 1950 they started the automotive control cables production.

Thanks to an engineering enhancement and customisation of the products promoted by the company owner, Sila continued to grow, becoming in 1985 the first company in Europe to develop and produce a complete gear-shifting system based on flexible cable technology.

Today SILA is a company developing manual transmission shifter systems, automatic transmission shifter systems and full-by-wire shifting solutions.

## 1.2 Shifting systems

The shifting system is a component used in the automotive industry to convert the driver's will into an action on the vehicle. The system is mainly composed by a selector and mechanical cables linked to the gearbox of the vehicle.

The selector can be a lever, a rotary or a mono-stable selector, and it is used by the driver to choose the desired driving mode, in automatic transmission shifter, or to select the needed gear in manual transmission shifter.

The aim of the shifting system is to translate this input signal from the driver into the movement of the mechanical cables acting on the gearbox that will implement certain changes on the vehicle dynamics.

The mechanical cables used to operate on the gearbox are special cables based on flexible cable technology, which is an important development of the already existing technology based on rod linkage. These are push-pull cables that guarantee better shiftability, noise reduction and improve comfort on the vehicle.

Depending on the type of the vehicle transmission, the mechanical cables of the shifting system are different.

For a manual transmission gearbox two cables will be needed, one for shifting and the other for the selection, but for an automatic transmission only one cable is required.

For an automatic transmission gearbox, the shifting system task is to switch between the different driving modes: P, R, N, D.

In order to do so, the mechanical cable is moved longitudinally by means of a suitable mechanical system activated by the driver's power stroke or an electrical motor depending on the shifting system technology. The longitudinal movement of the cable is able to apply a torque on a leverage present on the vehicle gearbox changing its angular position. The position of this lever corresponds to a certain driving mode.

As for many other automotive components, also the shifting systems are changing from a purely mechanical to electronic actuation, creating the shift-by-wire shifting solutions opposing the shift-by-cable shifting solutions mentioned above.

## Chapter 2

# Mechanical prototype and functional requirements

The shifting system under analysis is an automatic transmission system. It is composed by a selector that communicates through the CAN communication protocol to the shifting system the desired driving mode selected by the driver.

The shifter is an electromechanical item composed by an electrical DC motor that through a transmission moves the mechanical cable into the desired position moving the lever present on the gearbox of a certain angle. The gearbox will then operates certain adjustment in the vehicle dynamics.

In this first development phase of the project, the considered driving modes are P (parking) and not P (N, R, D without further distinction). For this reason the shifting system will also be called "Park actuator".

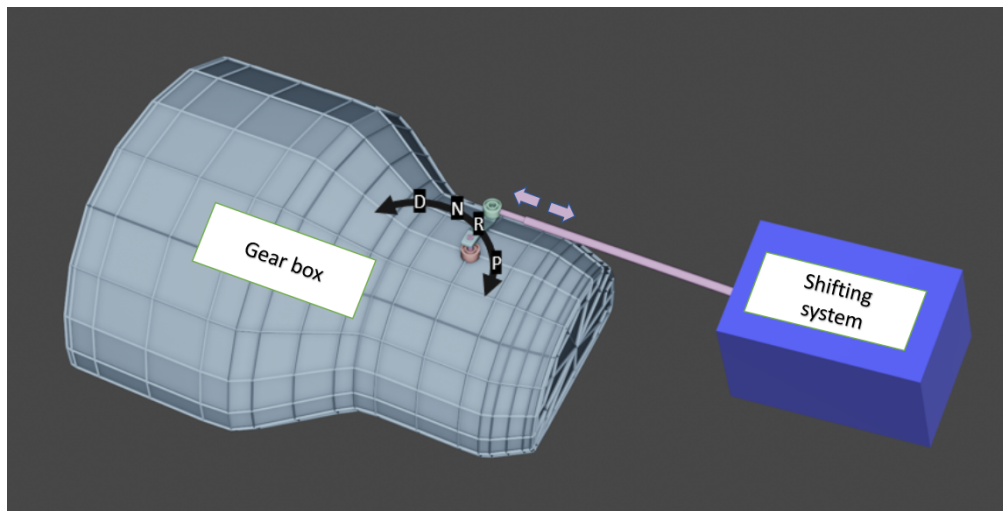


**Figure 2.1:** Park actuator shifting system

## **2.1 Mechanical prototype**

In order to achieve the customer functional requirements, a purely mechanical prototype of the shifting system was developed by our colleague.

The object was designed based on benchmarking procedure, old prototype versions already implemented inside the company and the customer requirements. He was careful to choose already existing components in order to get a less expensive and easily industrialisable solution.

The prototype, shown in Figure 2.2, consists in the following components:

- Electrical motor
- Helicar gear transmission
- Screw-nut transmission system
- First runner connected directly to the transmission
- Second runner on which is located the housing for the mechanical cable to be moved
- Spring for the emergency function between the two runners mentioned above
- Electromechanical retaining system formed by rods, fork, bridge and electro-magnet beneath the support above the bridge

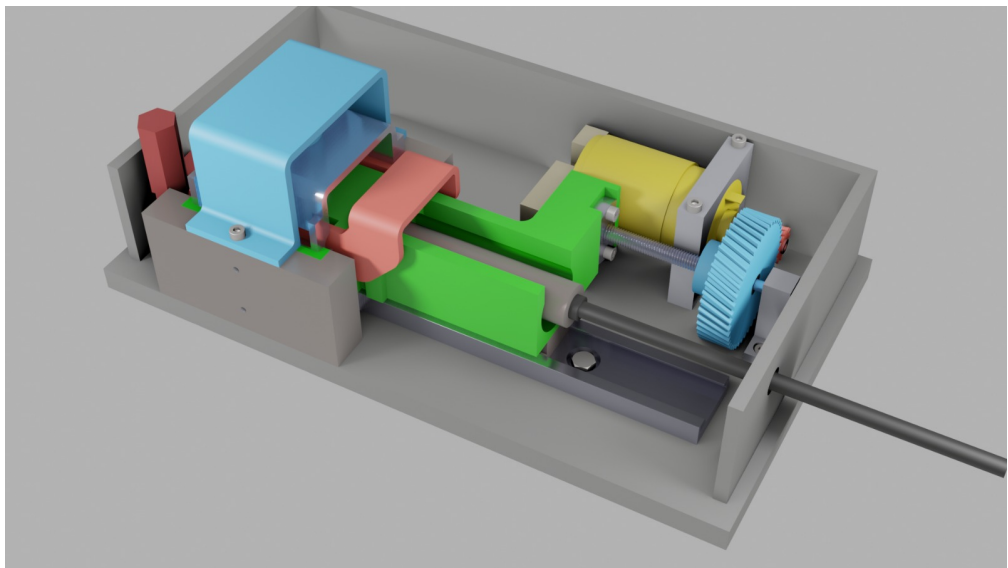


**Figure 2.2:** Park actuator prototype

### 2.1.1 Electrical motor

The electrical motor chosen by the colleague is a permanent magnet brushed DC motor, suitable for the loads it has to overcome.

The informations in the motor datasheet are the following:

Rated voltage	12 V
Rated current	8 A
Rated speed	7,357 rpm
No load current	0.43 A
No load speed	9,000 rpm
Torque constant	12.6 mNm/A
Motor resistance	0.32 $\Omega$

**Table 2.1:** Motor datasheet

This type of motor can be driven through a voltage driving strategy. The software and hardware needed to drive it will be discussed further on in this document.

### 2.1.2 Transmission and runners

The whole transmission system is composed by the helical gear transmission and the screw-nut transmission system.

Since the mechanical cable is moved forward and backward from the two position P and not P, the transmission is designed to be reversible and suited for the loads the system has to overcome.

The two transmissions are characterized by the following transmission ratio and efficiency:

Transmission	Transmission ratio	Efficiency
Helical gear	3.75	0.947
Screw-nut	$8.08 \times 10^{-4}$	0.56

**Table 2.2:** Transmission data

Connected to the transmission there is the first runner that is the one the electrical motor moves.

The second runner on which the housing for the mechanical cable is located is put in motion by the first runner when the two are kept integral by the retaining system.

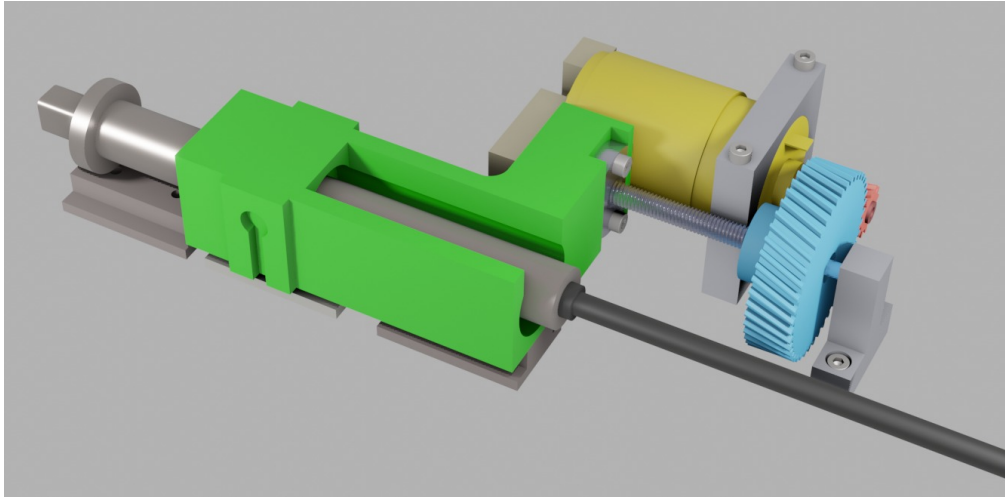


**Figure 2.3:** Runners configuration

### **2.1.3 Retaining system**

To satisfy the functional requirements, an electromechanical retaining system is present.

The system is composed by a fork, two rods, a bridge and an electromagnet (not shown in the picture below).

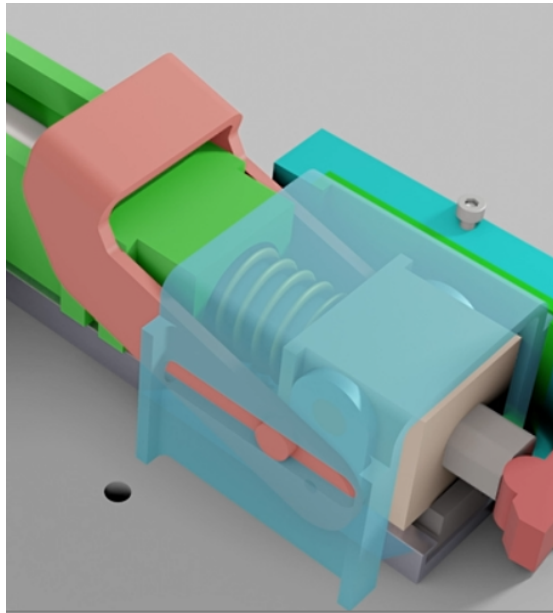


**Figure 2.4:** Retaining system

The aim of these components is to keep the spring compressed during the normal operating mode and to connect the two runners making their motion integral. The electromagnet, which is located above the bridge, is a 12 V component with an absorbed current of 0.25 A and it is able to attract up to 50 N.

## **2.2 Functional requirements**

The aim of the park actuator is to move the mechanical cable in two different positions: P and not P.

Besides this main function there is an innovative "Emergency function" feature that consists in returning the cable in the P position if an electrical fault occurs.

### **2.2.1 Normal operating mode**

The first operation the park actuator must perform is the preparation for the emergency function.

When the vehicle engine is off, the mechanical cable is in the P position.

At the opening of the vehicle door, the system loads the spring between the two runners supplying the electrical motor, moving the first runner connected to the transmission. The second runner on which is located the housing of the mechanical cable is held in place in P position by a mechanical block.

This way, the spring present between the two runners is compressed.

The movement of the first runner, on which the fork is connected, causes also the rotation of the rods on the second runner resulting in a change of inclination of the fork itself and therefore in an upward movement of the bridge.

The total "spring loading" sequence ends when the bridge reaches the supplied electromagnet that will keep the retaining system in position resulting in a ready-to-work system with the spring correctly loaded and the two runners in a configuration in which they move in solidarity as shown in Figure 2.5.

The duration of the "spring loading" phase is not specified by the customer but it is required that it does not lead to a waiting of the human driver before disengage the P mode.

The park actuator is now ready to operate the engaging and disengaging P mode phase by moving the mechanical cable in the P and not P position based on the signal received by the selector on which the human driver operates.

The electrical motor is therefore correctly supplied in order to move the cable in the right direction in the right timing.

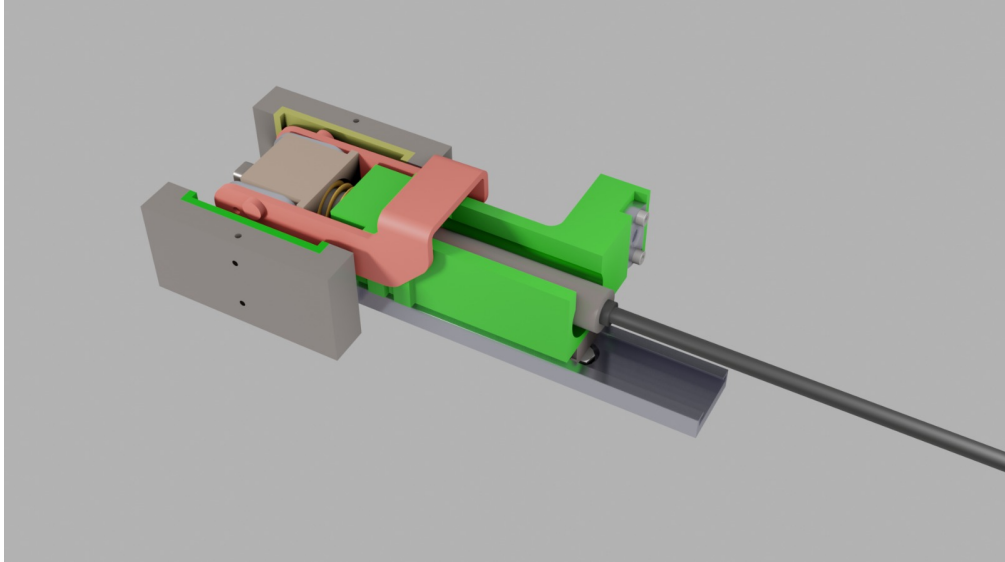


**Figure 2.5:** Runners configuration after the spring loading phase

## 2.2.2 Emergency mode

This is an additional function required by the customer.

In case of an electrical fault, the system must be able to return the mechanical cable in the P position.

This is the motivation that justifies the presence of the spring.

In case of electrical fault the electromagnet, that is connected to the 12 V vehicle battery, losses its power supply resulting in a release of the mechanical retaining system discussed above that leads to spring relaxation and the two runners not be integral anymore.

The relaxation of the spring causes the motion of the two runners: the first one connected to the transmission is free to move forward thanks to the reversibility of the transmission system. The second runner with the housing of the mechanical cable is forced to move backward returning the cable in the P position.

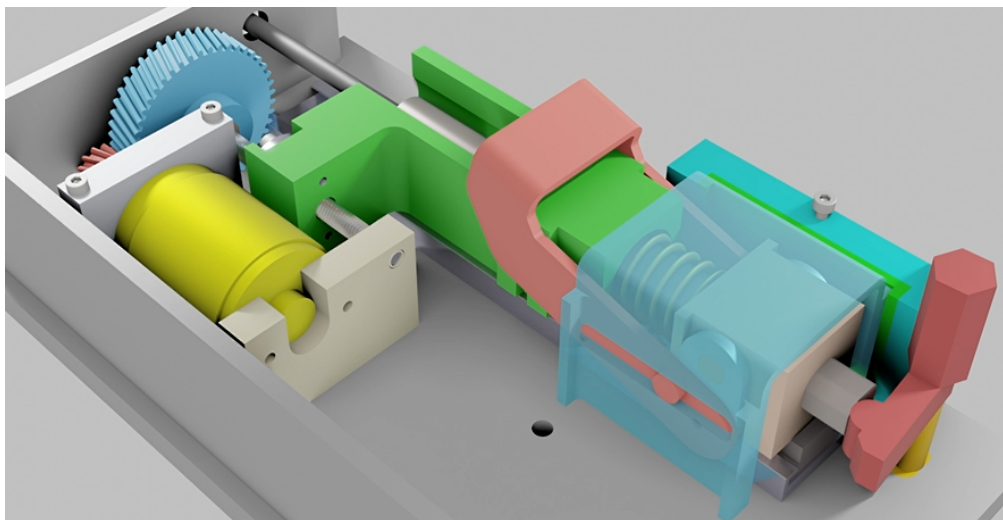


**Figure 2.6:** Shifting system in the released spring configuration

## Chapter 3

# Model based design approach

To reach our goal of prototype handling, in agreement with the company, the model based design approach was chosen.

The model based approach is a strategy that is based on the creation of a virtual model of a system. This virtual model is built to describe the main features of the system under analysis.

Based on the aim, different system features are highlighted and a suitable modelling strategy is chosen.

Therefore there are several different possibilities to model the same system.

Moreover, the model based approach is very useful, in particular at the beginning of the design phase, since it lets the developers to study and test different design solutions easily, without the need of physical prototypes.

In our case, the work is focused on the functional characteristics of the system and a Simulink model is implemented.

Simulink is a Matlab tool for simulation and modelling that focuses on the creation of schemes based on blocks.

The features of the system are represented by their transfer functions built with the appropriate block or inter-block connection. The blocks are then connected together to implement the virtual model of the system.

The obtained virtual model is used for simulation in order to study the system dynamics, better understand the behaviour of the modeled components and to design a control strategy to drive the DC electrical motor in order to satisfy the handling requirements.

To implement the model, the main characteristics of the shifting system must be identified and their behaviour correctly modeled.

The highlighted system features are:

1. DC electrical motor
2. Transmission
3. Internal loads due to the prototype itself
  - (a) Static and dynamic friction of the runners
  - (b) Spring load
4. External load to engage/disengage the park actuator

In this chapter it will be analyse the modelling of the different components while the values of the quantities involved will be discuss in Chapter 5 "Model validation".

### 3.1 DC Motor model definition

The main component to be modeled is the electrical motor.

The electrical motor is a machine able to convert electrical energy into mechanical energy.

The chosen motor is a brushed permanent magnet DC motor. It is a direct current machine that does not need an excitation circuit because a constant magnetic flux, needed by the motor to work properly, is produced by the permanent magnet present in the machine itself.

Its behaviour can be summarize by the electrical scheme in Figure 3.1.

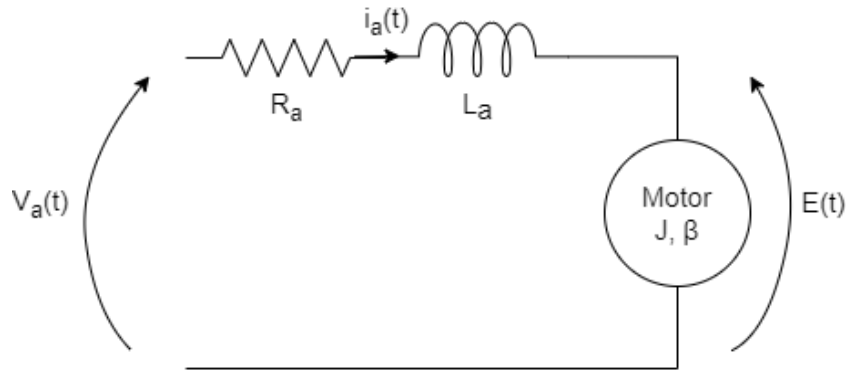


**Figure 3.1:** DC motor electrical scheme

Starting from the electrical model is possible to write the electrical equation of the DC machine, Equation 3.1, that together with the mechanical equation, Equation 3.2, described the dynamical behaviour of a DC electrical motor.

$$V_a(t) = R_a \cdot i_a(t) + L_a \cdot \frac{di_a(t)}{dt} + E(t) \quad (3.1)$$

$$T_m(t) = T_r(t) + \beta \cdot \omega(t) + J \cdot \frac{d\omega(t)}{dt} \quad (3.2)$$

$$E(t) = k_v \cdot \omega(t)$$

$$T_m(t) = k_t \cdot i_a(t)$$

The quantities that characterise the electrical machine are:

**Electrical quantities :**

$V_a(t)$  [V] is the voltage supplied to the motor

$E(t)$  [V] is the electromotive force (e.m.f) generated by the motor

**Electrical parameters :**

$R_a$  [ $\Omega$ ] is the motor resistance

$L_a$  [H] is the motor inductance

**Mechanical quantities :**

$T_m(t)$  [N m] is the mechanical torque generated by the motor

$T_r(t)$  [N m] is the external resistant torque applied to the motor

$\omega(t)$  [rad/s] is the rotor angular velocity

**Mechanical parameters :**

$J$  [kg m<sup>2</sup>] is the rotor inertia

$\beta$  [Nm s/rad] is the viscous friction coefficient

**Motor constant :**

$k_v$  [V s/rad] is the e.m.f. constant

$k_t$  [Nm/A] is the torque constant

It is important to remark that  $k_v = k_t = k \cdot \phi$  where  $k$  is a machine constant and  $\phi$  is the machine flux

From the parameters above is possible to define the electrical time constant  $\tau_a$  [s] and the mechanical time constant  $\tau_m$  [s]:

$$\begin{aligned}\tau_a &= \frac{L_a}{R_a} \\ \tau_m &= \frac{R_a \cdot J}{k_t \cdot k_v}\end{aligned}\tag{3.3}$$

To compute the transfer function that describe the DC motor behaviour, the equation Equation 3.1 and Equation 3.2 are converted from continuous time into *Laplace* domain obtaining:

$$V_a(s) = R_a \cdot i_a(s) + s \cdot L_a \cdot i_a(s) + E(s) \quad (3.4)$$

$$T_m(s) = T_r(s) + \beta \cdot \omega(s) + s \cdot J \cdot \omega(s) \quad (3.5)$$

$$E(s) = k_v \cdot \omega(s)$$

$$T_m(s) = k_t \cdot i_a(s)$$

From these equations it derives the DC motor transfer function, Equation 3.6, with input the supplied voltage  $V_a(s)$  and output the angular velocity  $\omega(s)$  as the external torque, as it will be discussed further on, is dependant on the runners displacement and so it is part of the system behaviour.

$$\frac{\omega(s)}{V_a(s)} = \frac{\frac{1}{k_v \cdot \tau_m \cdot \tau_a}}{s^2 + \frac{s}{\tau_a} + \frac{1}{\tau_a \cdot \tau_m}} \quad (3.6)$$

The denominator can be rewritten as:

$$s^2 + \frac{s}{\tau_a} + \frac{1}{\tau_a \cdot \tau_m} = 1 + s \cdot \tau_m + s^2 \cdot \tau_a \cdot \tau_m \approx (1 + s \cdot \tau_a) \cdot (1 + s \cdot \tau_m)$$

Therefore the DC motor is a second order, BIBO stable system with two negative real separated poles: the faster electrical pole in  $s = -\frac{1}{\tau_a}$  and the slower mechanical pole in  $s = -\frac{1}{\tau_m}$ .

The electrical motor frequency response, Figure 3.2, shows a behaviour similar to a low pass filter, which is an aspect the must be taken into account when choosing the PWM frequency for the voltage driving as it will be discuss later in Chapter 4 "Hardware implementation".

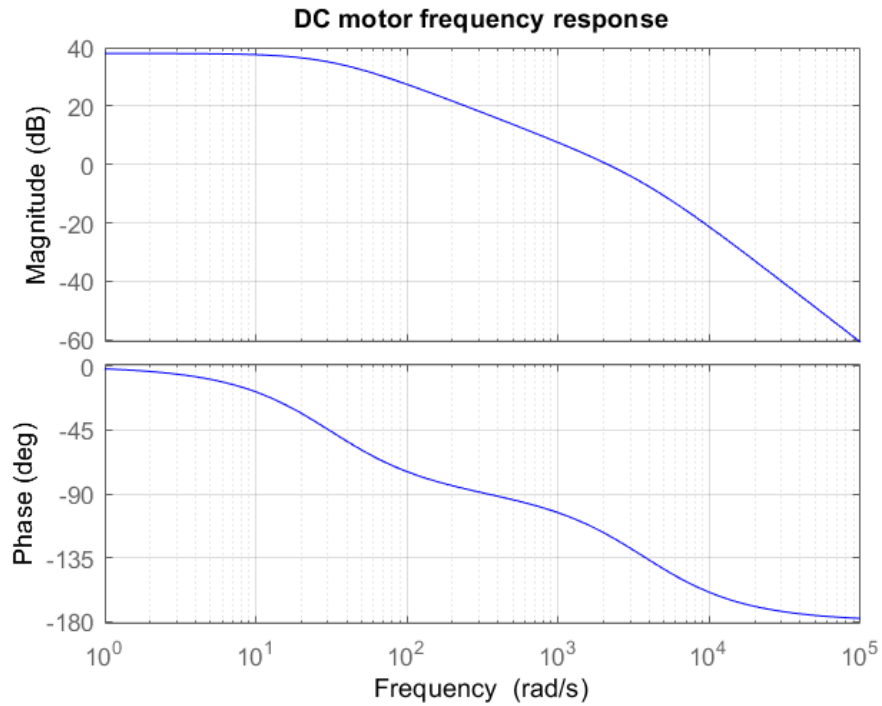


Figure 3.2: Frequency response of the DC motor

### 3.1.1 Electrical motor block scheme

It is now possible to build the Simulink block scheme having as inputs the supplied voltage  $V_a(s)$  and the external torque  $T_r(s)$  and as output the rotor angular velocity  $\omega(s)$ .

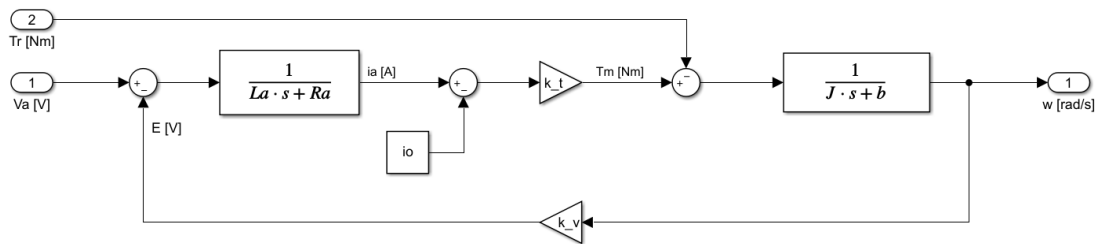


Figure 3.3: DC motor continuous time model

The blocks used to create the model are:

- transfer function block to implement the electrical equation, Equation 3.4, and the mechanical equation, Equation 3.5



- Gain block of value  $k_v$  or  $k_t$



- Constant block to implement a first approximation of the no load current  $i_0$



The model in Figure 3.3 is a first approximation of the DC motor, easy to build but too poor to simulate the real time behaviour of the DC motor so it has to be improved.

In order to improve it, the model needs to be a discrete time model.

To implement it in discrete time, the equations are converted from the *Laplace* domain into the *z-transform* domain.

The transformation for the electrical transfer function from *Laplace* domain into *z-transform* domain is operated as follows:

$$\begin{aligned}\frac{i_a(s)}{V_a(s) - E(s)} &= \frac{1}{s \cdot L_a + R_a} \\ i_a(s)(s \cdot L_a + R_a) &= V_a(s) - E(s) \\ i_a(s) \cdot R_a + s \cdot i_a(s) \cdot L_a &= V_a(s) - E(s)\end{aligned}$$

In continuous time it becomes:

$$i_a(t) \cdot R_a + L_a \cdot \frac{di_a(t)}{dt} = V_a(t) - E(t)$$

Finally in the discrete time it is:

$$\begin{aligned}R_a \cdot i_a(i) + L_a \cdot \frac{i_a(i) - i_a(i-1)}{\Delta t} &= V_a(i) - E(i) \\ i_a(i) &= ((V_a(i) - E(i)) + \frac{L_a}{\Delta t} \cdot i_a(i-1)) \cdot \frac{1}{R_a + \frac{L_a}{\Delta t}}\end{aligned}$$

Where  $\Delta t$  is the time between the two considered time instants  $i$  and  $i - 1$ . It is set to be  $\Delta t = step\_size$ . The  $step\_size$  is the time step that is used by Simulink in the discrete time simulation to compute the dynamic evolution of the system and the criterion used to choose its value will be discussed in Chapter 4 "Hardware implementation".

The discrete equation is then implemented through blocks as shown in Figure 3.4. The used blocks are gain blocks and a new block called "unit delay" which applied to a signal sample and hold the quantity with one sample period delay.

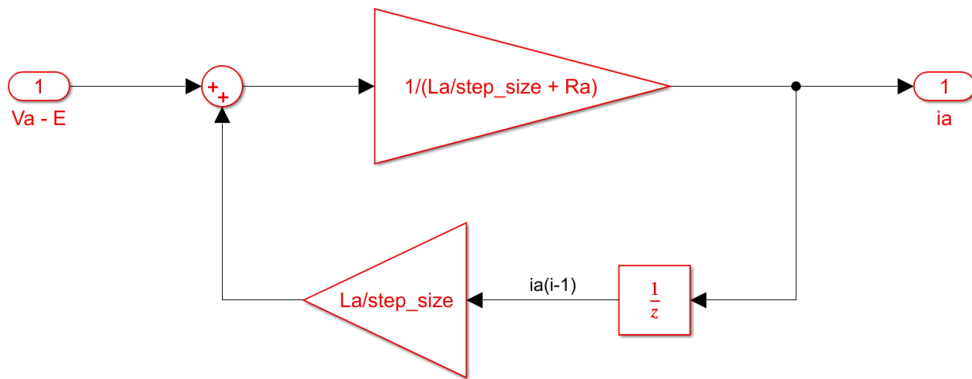


**Figure 3.4:** Discrete electrical block

The same approach is applied to the transformation of the mechanical equation from *Laplace* domain into *z-transform* domain creating the discrete block scheme in Figure 3.5.

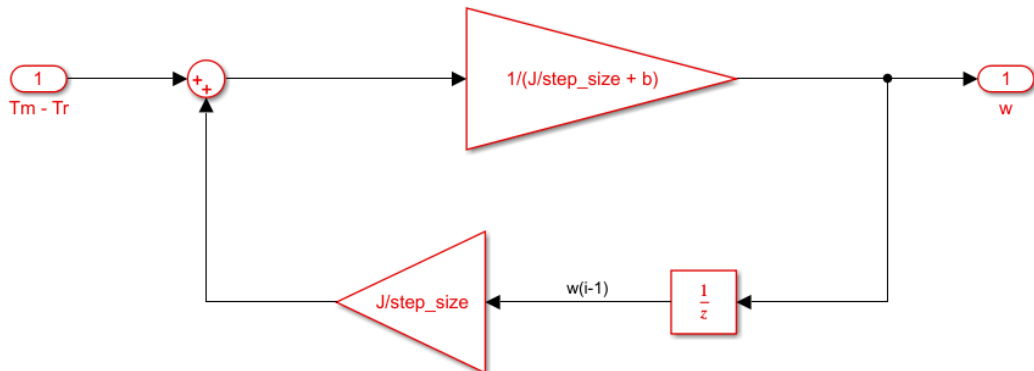


**Figure 3.5:** Discrete mechanical block

A final enhancement in the motor model is about the no load current block. The no load current  $i_0$  is the current absorbed by the DC motor that is not converted into mechanical torque  $T_m$  since the motor is subject to internal dissipation such as the bearing friction.

The no load current  $i_0$  acts like a threshold the absorbed current  $i_a$  has to exceed in order to produce mechanical torque  $T_m$  that can be use to overcome the external loads.

The value of  $i_0$  increases with  $i_a$  until it reaches a threshold and then remains constant.

$$i_0 = \begin{cases} i_a & \text{when } i_a \leq i_0 \\ i_0 & \text{when } i_a > i_0 \end{cases}$$

To model this behaviour, "if" block and "if - action" blocks are used resulting in this block scheme.

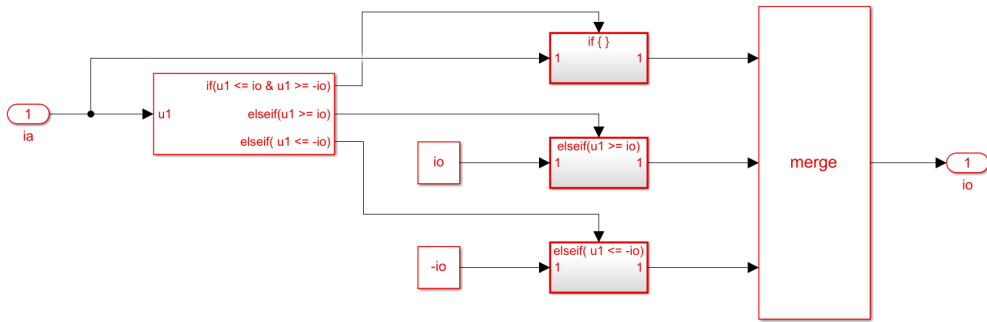


Figure 3.6: No load current calculation

The final discrete time block scheme for the DC motor, ready to use in simulation and design purpose is the one shown in Figure 3.7.

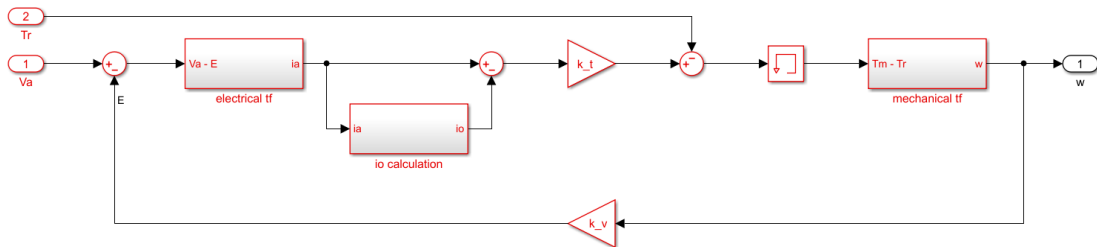


Figure 3.7: DC motor discrete time model

### 3.2 Transmission block scheme

Another important feature of the park actuator is the transmission system composed by the helical gear transmission and the screw-nut transmission system.

The transmission system is the component that allows the propagation and the transformation of the motion from the rotor rotational motion to the longitudinal motion of the runners and so the mechanical cable linked to one of them. The block scheme is built to represent this behaviour.

As for the DC motor, a first model in continuous time is created and discretized in a second moment.

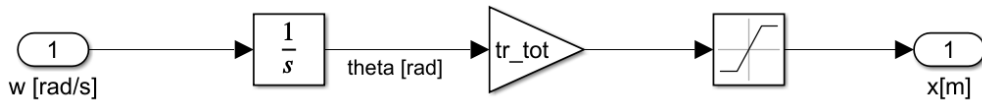


**Figure 3.8:** Transmission continuous time model

The input of this block is the angular velocity of the motor  $\omega$  [rad/s] while the output is the longitudinal displacement of the runners and so the mechanical cable  $x$ [m].

The blocks used to define the block scheme are the following:

- Integrator block to convert the rotor angular velocity  $\omega$  [rad/s] into the rotor angular displacement  $\Theta$  [rad]. For the discrete time integrator also the sample time  $T_s$  that is set equal to the simulation step time is taken in to account.



**Figure 3.9:** Continuous time integrator block (on the left) and discrete time integrator block (on the right)

- Gain block to apply the total transmission ratio of the whole transmission system.

The total transmission ratio  $t_{r_{tot}}$  is computed using the values in the table Table 2.2.

$$t_{r_{tot}} = \frac{8.08 \times 10^{-4} \text{ m/rad}}{3.75} = 2.16 \times 10^{-4} \text{ m/rad}$$

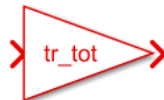


**Figure 3.10:** Gain block

- Saturation block to represent that the longitudinal displacement available in the mechanical prototype has physical limits

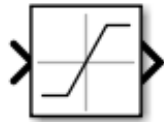


**Figure 3.11:** Saturation block

The final discrete time scheme to represent the transmission is the following:

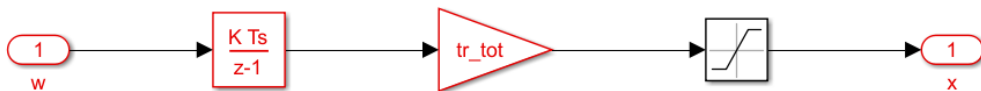


**Figure 3.12:** Transmission discrete time model

### 3.3 Loads block scheme

In the previous section, the DC motor block scheme was defined. This block receive as input the supplied voltage  $V_a$  and the resistant torque  $T_r$ .

The load block scheme is added in the total system model to compute the resistant torque  $T_r$  that acts on the DC motor.

Based on the specific operating condition in which the park actuator is working, the resistant torque  $T_r$  assumes a different behaviour.

The resistant torque applied to the DC motor originates from different loads that can be distinguished in:

**Internal loads** : these loads are generated by the prototype mechanics and therefore internal to it

**External loads** : there loads are generated by components external to the shifting system such as the mechanical cable and the gearbox connected to the actuator

The internal loads are the ones coming from the static and dynamic friction of the runners, the transmission and the other moving parts.

Another source of internal load is the spring for the emergency function. During the spring loading phase, the motor has to overcome the elastic force that the spring generates during its compression.

It is very important to model the internal loads in the best possible way in order to have a good description of the shifting system behaviour.

The external loads instead are the ones generated by the mechanical cable and the gearbox. In order to engage or disengage the driving mode on the gearbox, the shifter moves the leverage on the gearbox and in order to do so it has to overcome a resistant force profile that depends on the cable displacement and it is different from one gearbox to an other.

Simulating these loads is important for the control system design phase in order to achieve the functional requirements on the system in terms of supplied voltage and handling timing.

### 3.3.1 Static and dynamic friction modelling

The friction is a resistant force always presents when motion is involved. In the park actuator prototype, friction is present in the electrical motor, in the transmission system, between the runners and their guide.

The friction inside the DC motor is caused mainly by the bearings and the rotational motion of the rotor. These contributions have been modeled in the electrical motor scheme block.

The bearing friction has been taken into account by introducing in the scheme the block of the no load current  $i_0$  while the friction due to the rotor motion, that generates a contribution proportional to the angular velocity, is take into account by the presence of the viscous friction coefficient  $\beta$  in the mechanical equation, Equation 3.2, of the DC motor.

The friction in the transmission system is due to the physical contact between teeth of the gears in the helical gear transmission and between the screw and the nut in the screw-nut transmission system. These contacts during the movement generates friction.

These contributions are taken into account by the efficiency coefficients of the transmission systems and they are put into the system model using a simple gain block as it will be shown later.

The friction due to the runners moving in their guide needs to be modeled in a specific block that is added to the final system model.

Two types of friction are considered: the static friction and the dynamic friction. The static friction force  $F_s$  is the resistant force that the applied force has to overcome in order to move a body while the dynamic friction force  $F_d$  is a resistant force present until the body is in motion. As all the other friction forces, it opposes to the motion.

They are computed as follows:

$$F_s = \mu_s \cdot N$$

$$F_d = \mu_d \cdot N$$

where  $\mu_s$  is the static friction coefficient and  $\mu_d$  is the dynamic friction coefficient that depend on the material the runners and the guide are made off.

$N$  is the normal force that depends on the mass of the runners.

Since  $\mu_d < \mu_s$ , the static friction force is always greater than the dynamic friction force.

These friction forces translate into resistant torques  $T_r$  acting on the DC motor.

More specifically, the resistant torque  $T_r$  is equal to

$$T_r = \begin{cases} T_m & \text{when } \omega \approx 0 \\ T_{r_{friction}} & \text{when } \omega \neq 0 \end{cases}$$

When the runners are not in motion, so  $\omega = 0$ , the system is in a static condition and so the generate torque and the resistant torque are equal and opposite since  $T_m + T_r = 0$ .

During this phase the DC motor starts to increase the absorbed current  $i_a$  in order to overcome the friction load and so the generated torque  $T_m$  increases. The absorbed current  $i_a$  increases until the generated torque  $T_m$  reaches the values of torque generated by the static friction force. After this, the runners start moving, the system is in the condition where  $\omega \neq 0$ . During this motion phase, the resistant torque is the one generated by the dynamic friction forces.

This logic is represented in the block scheme as shown in the following picture. The used block are the "if" and "if action" blocks. In the if block a hysteresis logic on  $\omega$  is implemented to recreate the condition  $\omega \approx 0$ .

The value of  $\omega_{hysteresis}$  is less than 1 rad/s.

Inside the scheme, the friction is already expressed as resistant torque applied to the DC motor.

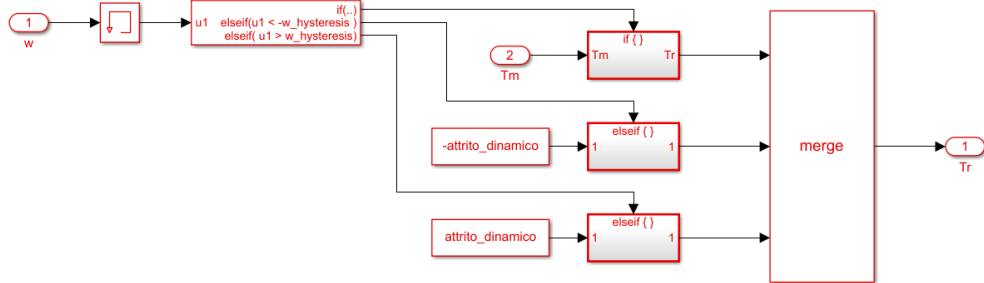


Figure 3.13: Static and dynamic friction block scheme

Inside the first "if action" block that returns as output  $T_r = T_m$ , a subsystem is implemented in order to obtain the following logic:

$$T_r = \begin{cases} -T_m & \text{when } \omega < 0 \\ T_m & \text{when } \omega > 0 \end{cases}$$

In this way the torque generated by the dynamic friction force is always opposing the torque generated by the DC motor.

The subsystem is the one shown in the picture above.

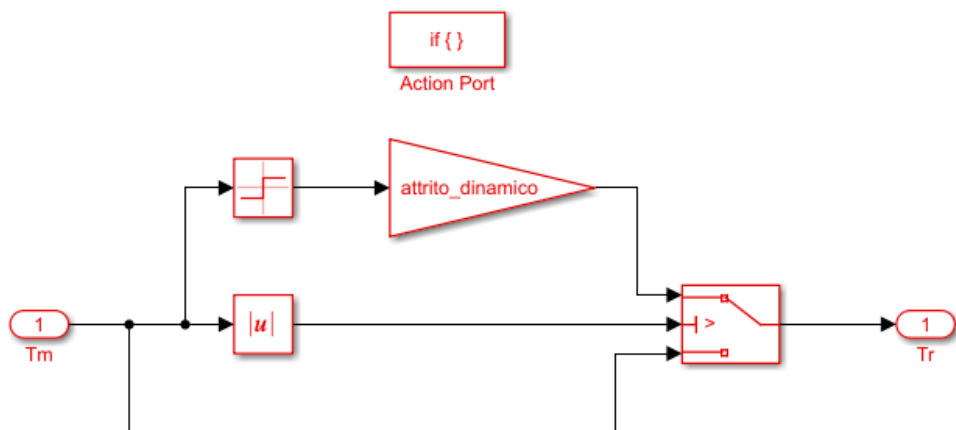
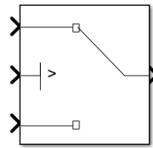


Figure 3.14: Dynamic friction subsystem

The used blocks in this subsystem are:

- Gain block
- Switch block: Pass through input 1 when input 2 satisfies the selected criterion; otherwise, pass through input 3.

The criteria for control port 2 are  $u_2 \geq Threshold$ ,  $u_2 > Threshold$  or  $u_2 \approx 0$ .



**Figure 3.15:** Switch block

- Absolute value block: returns as output the absolute value of the input



**Figure 3.16:** Abs block

- Sign block: returns as output 1 for positive input, -1 for negative input, and 0 for 0 input

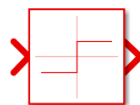


**Figure 3.17:** Sign block

### 3.3.2 Spring load modelling

The other important load internal to the park actuator prototype to model is the one produced by the spring for the emergency function.

When the system is in the normal operating mode, the first action it has to implement is the preparation of the emergency function and it does it by compressing the spring located between the two runners.

During the compression the spring produces an elastic force that translates into an important resistant torque on the DC motor. For this reason it is essential to model this phenomenon in order to obtain a model that can be use to design a control strategy to drive the motor to overcome this force and realise the required action of spring compression.

The elastic force  $F_{el}$  generated by the spring is a force proportional to the linear displacement  $x$  through the elastic coefficient of the spring.

The elastic coefficient is determined by the mechanical characteristics of the spring. In the park actuator prototype the spring, even before its loading, has an initial compression  $x_0$ , so the elastic force can be expressed as:

$$F_{el}(t) = k_{el} \cdot (x(t) + x_0)$$

The elastic force  $F_{el}$  needs to be converted into a resistant torque acting on the DC motor. This physical transformation is operated by the screw-nut transmission system.

A force, such as the elastic force, applied to the runner which is rigidly connected to the nut, generates a torque  $T_{screw}$  on the screw according to Equation 3.7.

$$T_{screw} = \frac{F_{el} \cdot R_{screw-nut}}{\eta_{screw-nut}} \quad (3.7)$$

where  $R_{screw-nut}$  is the transmission ratio and  $\eta_{screw-nut}$  is the screw-nut transmission system efficiency.

Moreover, in the transmission system the helical gear transmission is present and the effect it generates is to propagate the motion with a certain transmission ratio  $i_{gear}$  and propagate the resistant elastic resistant torque with a certain efficiency  $\eta_{gear}$ .

In order to represent correctly this behaviour, the elastic resistant torque is computed as:

$$T_{el} = C \cdot F_{el}$$

where  $C$  is a coefficient defined as:

$$C = \frac{R_{screw-nut}}{i_{gear} \cdot \eta_{screw-nut} \cdot \eta_{gear}} \quad (3.8)$$

The final block scheme that represents the spring behaviour during the spring loading phase is the following.

The used blocks are gain blocks and constant block.

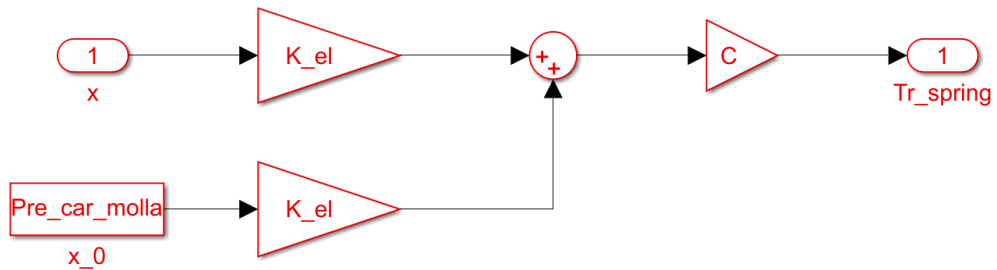


Figure 3.18: Spring block scheme

### 3.3.3 External gearbox load modelling

The main purpose of the park actuator is to switch the lever on the gearbox to a certain angle to engage or disengage the P mode.

To do so the actuator has to overcome the resistant force the gearbox opposes.

The resistant force  $F_{gearbox}$  is a variable load that depends on the angular displacement of the gearbox lever that corresponds to a longitudinal displacement of the mechanical cable moved by the shifting system.

The values of the force  $F_{gearbox}$  depend on the specific gearbox on which the shifter is operating, but the force profiles are similar.

Moreover, the values of the force  $F_{gearbox}$  also depend on the position of the vehicle in the road; disengage the P mode in a vehicle parked on a slope will require more effort than to do it in a vehicle on a level road.

The two force profiles that are analysed in this thesis are from two different gearboxes.

The first one is the one the customer required the shifting actuator for but it was not available for the testing phase. However thanks to the model based approach we chose, my colleague and I were able to overcome this problem.

The tests were run on a different gearbox, with different force values but similar profile. We needed only to make few adjustment on the load block scheme in the model and in the firmware and we were ready for the tests, thanks to the versability of this approach.

### Customer gearbox resistant force modelling

In the customer specifications document, the resistant force to disengage the P mode, so to do the movement from P to not P, was given with a graph without any data. The only available informations are the maximum force and the total displacement from P to not P in terms of mechanical cable displacement .

Based on these informations, an approximation of the force  $F_{gearbox}$  is made.

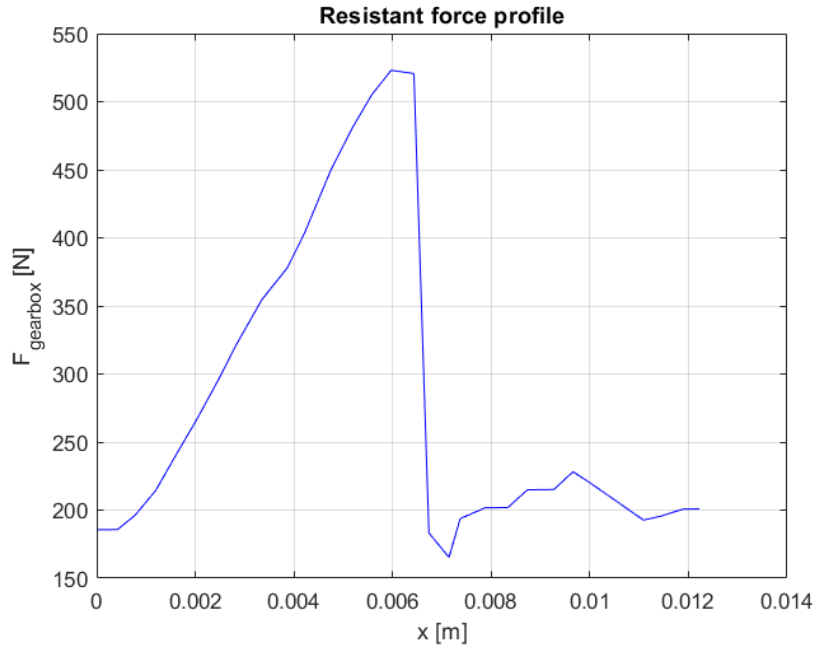


**Figure 3.19:** Force profile to disengage the P mode

A further approximation of this profile, Figure 3.20, is made by representing the profile as a straight line increasing from the initial value  $F_0$  up to the maximum value  $F_{max}$  during the first half of the total displacement  $x$ . In the second half instead, the force remains constant.

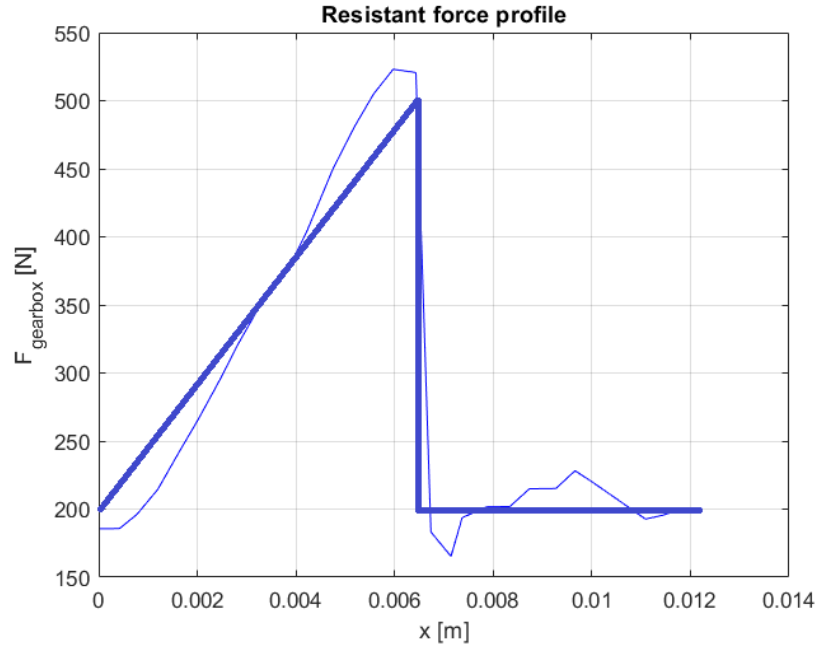


**Figure 3.20:** Approximation of the force profile to disengage the P mode

The equation of the straight line can be easily compute. The angular coefficient is defined as:

$$K_{StraightLine} = \frac{F_{max} - F_0}{\frac{x}{2}}$$

It follows that the approximation of  $F_{gearbox}$  is

$$F_{gearbox}(t) = \begin{cases} K_{straightLine} \cdot x(t) + F_0 & \text{when } x(t) \leq \frac{x}{2} \\ F_0 & \text{when } x(t) > \frac{x}{2} \end{cases}$$

Finally the resistant force has to be converted into the resistant torque applied to the DC motor by multiplying it times the constant  $C$ , that represents the transmission, defined in Equation 3.8.

$$T_{gearbox} = C \cdot F_{gearbox}$$

This gearbox resistant torque is modeled as shown above.  
The block scheme is implemented using the constant, switch and gain blocks.

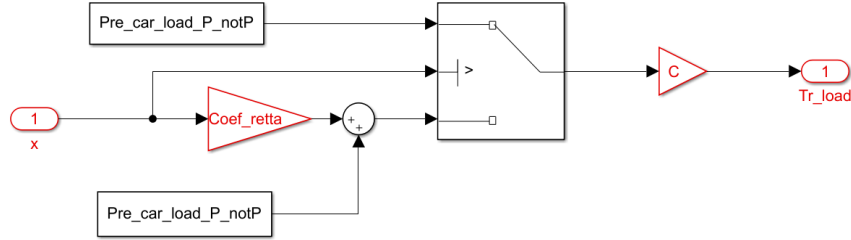


**Figure 3.21:** P mode disengaging block scheme

### Testing gearbox resistant force modelling

Due to the testing phase being run on a different gearbox already present in the company, a new model of the resistant force specific for the testing gearbox has to be built.

This time, even if the force profile is similar, the available data are given as resistant torque, instead of resistant force, with respect to the angular displacement, instead of the longitudinal displacement.

In order to keep the same structure used for the customer gearbox resistant force model, few adjustments have to be made.

First, the given resistant torque has to be converted into the resistant force to then convert it, through the transmission, into the torque applied to the DC motor. Second, the angular displacement has to be converted into the longitudinal displacement of the mechanical cable.

The first adjustment is the conversion of the resistant torque into the resistant force  $F_{gearbox}$ .

A mechanical torque  $T$  can be defined as:

$$\vec{T} = \vec{b} \wedge \vec{F}$$

where  $F$  is the force that generates the torque and  $b$  is of the lever arm which is the distance between the point of application of the force  $F$  and the lever fulcrum. The magnitude of  $T$  is

$$T = bF \sin \gamma$$

where  $\gamma$  is the angle between the vector  $F$  and the vector  $b$ .

In the shifting system, the mechanical cable in P position can be considered connected to the gearbox lever at a  $90^\circ$  angle so the torque magnitude is the product between the force  $F$  and the lever arm  $b$ .

Since the value of the lever arm on the gearbox is known,  $F_{gearbox}$  can be easily calculated.

The obtained  $F_{gearbox}$  has the same profile as for the other gearbox but a maximum value smaller than before.

The second adjustment to be done is the conversion of the gearbox lever angle displacement into the longitudinal mechanical cable displacement.

In order to do so, some considerations have to be done.

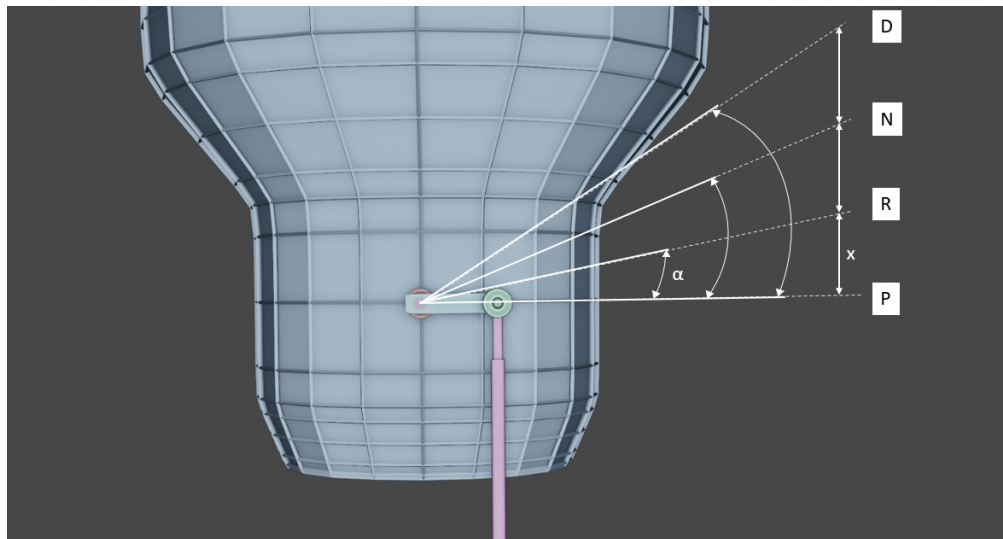


**Figure 3.22:** Gearbox selector

In Figure 3.22, the gearbox lever is shown. It is a simplified picture to help explain the trigonometric considerations.

As explained before, by changing the inclination  $\alpha$  of this lever it is possible to select the driving mode (P, N, R, D). To do so the mechanical cable of the shifting system has to be moved of a certain displacement  $x$ .

For this reason is essential to know the correlation between the angle  $\alpha$  and the displacement  $x$ .

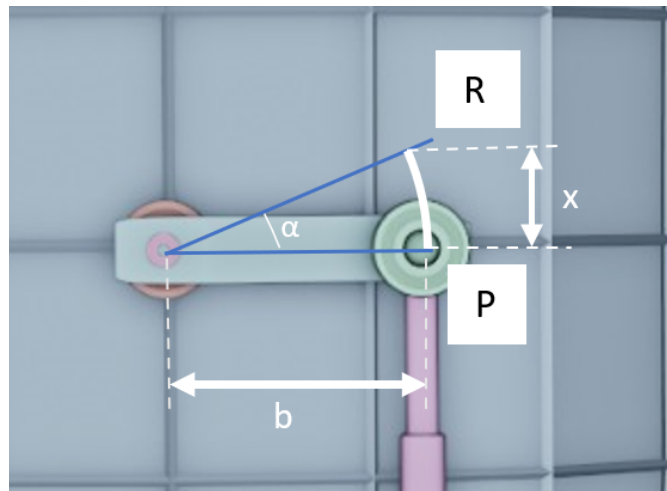


**Figure 3.23:** Gearbox selector -  $x$  calculation

In order to compute  $x$  for every  $\alpha$ , the displacement  $x$ , after converting  $\alpha$  into rad can be computed as:

$$x = b \cdot \sin \alpha$$

where  $b$  is the known lever length.

But the result that will be obtained is too poor, so for a better approximation the angle  $\alpha$  is divided in multiple parts, in our case two parts is sufficient.

$$x/2 = b \cdot \sin \alpha/2 \quad \rightarrow \quad x = 2 \cdot x/2$$

In this way, the resulting  $x$  is a better approximation on the arc of the circle the mechanical cable has to cover to switch the driving mode.

Now that the gearbox torque has been converted into the gearbox force  $F_{gearbox}$  and the angular displacement into the linear displacement  $x$ , it is possible to model the resistant torque that the gearbox imposes over the DC motor as it follows.

The model is implemented as for the displacement P - not P for the customer's gearbox.

Only the movement between the driving modes R and N is implemented because, due to the physical limits in the runners' guide in the prototype this is the movement that has been tested.

From R to N, the force  $F_{gearbox}$  is an increasing straight line until  $2/3$  of the displacement, then it remains constant at the initial value.

From N to R, the force  $F_{gearbox}$  is a decreasing straight line until  $2/3$  of the displacement, then it remains constant at the initial value.

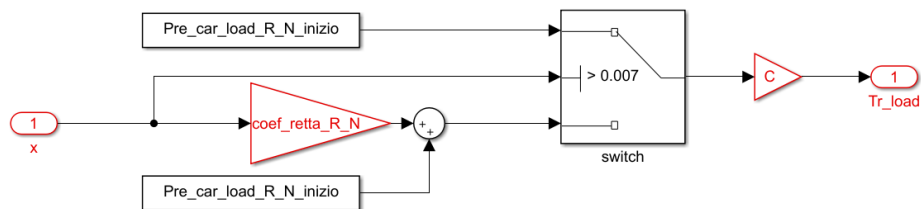


Figure 3.24: R - N mode switch block scheme

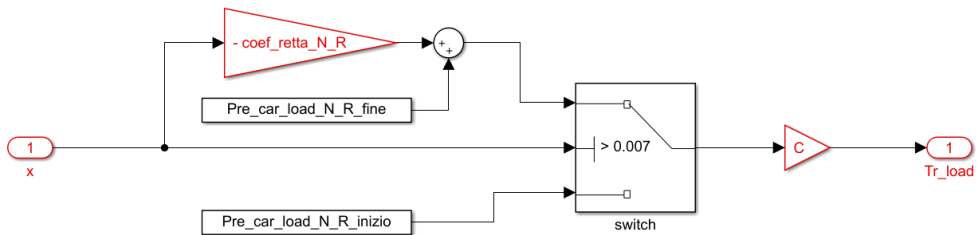


Figure 3.25: N - R mode switch block scheme

### 3.4 Complete plant model

Finally, after modelling all the main features of the shifting system, the complete Simulink model of the park actuator is built.

This model will be used to simulated the total behaviour of the park actuator and to design a suitable control system that, through the regulation of the supplied voltage, will generate the desired behaviour in terms of mechanical cable displacement.

The input of the system is the voltage supplied to the DC motor  $Va(t)$  while the output is the mechanical cable displacement  $x(t)$ .

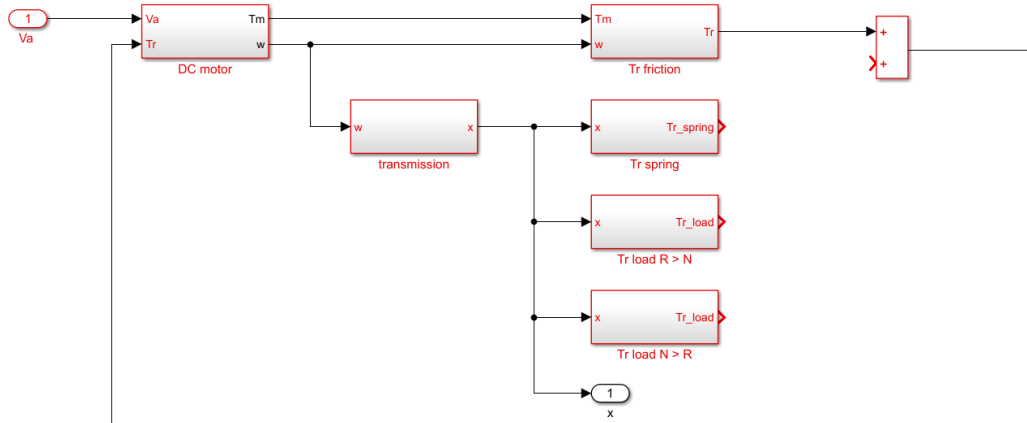


Figure 3.26: Shifting system block scheme

Starting from left there is the DC motor block which implements the DC motor block scheme in Figure 3.7. In cascade to it there are the friction block, that implements the scheme of the friction resistant torque that acts on the DC motor, Figure 3.13, and the transmission block that implement the transmission scheme block Figure 3.12.

In cascade to the transmission, there are three blocks that represent the working situation that the park actuator has to manage.

The first block represents the spring loading phase and inside of it these is the

spring scheme Figure 3.18.

The second block represents the movement from the R to the N driving mode and inside of it there is the R - N mode switch scheme shown in Figure 3.24.

The third block represents the movement from the N to the R driving mode and inside of it there is the N - R mode switch scheme shown in Figure 3.25.

## Chapter 4

# Hardware implementation

The main purpose of this master thesis is the correct handling of the mechanical prototype. In order to do so the electrical motor has to be supplied by the voltage profile computed by the control system based of the requirements on the different movements. To implement this procedure in real time on the physical prototype of the park actuator, the hardware part is essential.

The architecture to implement the handling of the shifting system in the different working conditions is the following shown in Figure 4.1.

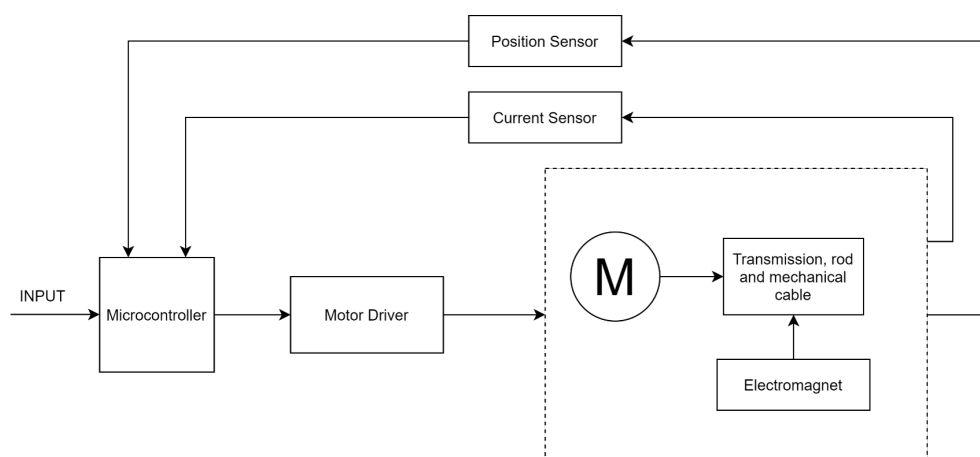


**Figure 4.1:** Hardware architecture

The hardware components are:

- The microcontroller to implement the logical part needed by the electronic system to work properly
- Sensors for measuring the physical quantities for control and testing purposes
- The motor driver to supply the DC motor
- the prototype to handle: DC motor, transmission and mechanical cable, electromagnet.

My colleague who is a master thesis student in electronic engineering took care of the hardware and firmware part, but is still very useful to do some considerations on this subject since the hardware components and their logic has to be taken into account while building the Simulink model of the shifting system in order to have a good approximation of what is implemented in real time by the physical system.

## **4.1 Microcontroller**

The microcontroller is the logic unit of the hardware part.

It is responsible for the acquisition of the human driver selection (at this stage of the work the selector is the button present on the board itself without the need of a CAN protocol), the implementation in real time of the control law, management of the motor driver component and data acquisition from the sensors.

The component my colleague did choose is the *STM32F411RE microcontroller* by *ST Microelectronics*, due to its software implementation independent from the model inside the same family, presence of debug tools and libraries, its compliance with project specifications and easy - to - use tools.

From the modelling point of view, its most important task is the implementation of the PWM square wave for the motor driver that will be discuss later in the document.

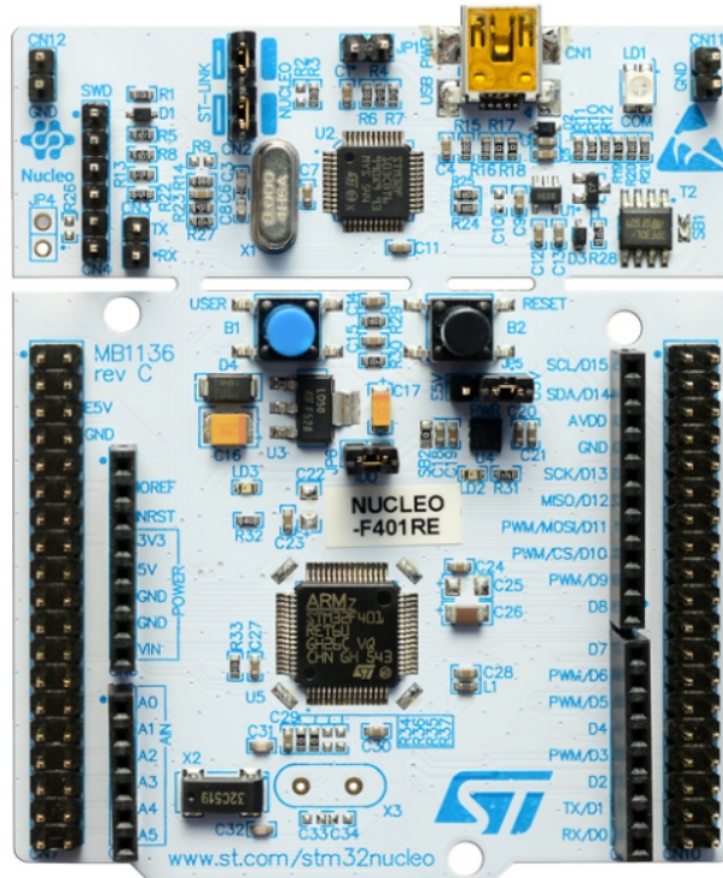


**Figure 4.2:** Microcontroller.

Image from <https://www.st.com/en/evaluation-tools/nucleo-f411re.html>

## 4.2 Sensors

The sensors are important components of the hardware architecture. They are fundamental to acquire data from the testing, to implement the feedback in the control strategy and to validate the model.

The used sensors are:

- Position sensor
- Current sensor

### 4.2.1 Position sensor

The position sensors are devices that acquired the angular or linear position of an object and transmit this information as a signal to the microcontroller.

They can be of different nature and working exploiting different physical phenomena.

In our application, the position sensor purpose is to provide the feedback of the variable under control in the control strategy. The control variable is the position of the mechanical cable.

After performing a trade off between costs, easiness of use - easiness of installation and performances, a resistive sensor was chosen. It is shown in Figure 4.3.

The sensor is a linear potentiometer by the company *Bourns* with a stroke of 30 mm. It is an analogical device that, depending on the position of its lever, produces a voltage signal that, by means of a analog/digital converter (ADC), is interpreted by the microcontroller. It has a sensitivity of 7  $\mu\text{m}$  and an uncertainty of 20% of the measure. The sensitivity is determined by the number of bits used by the ADC.

The chosen number of bits is 12 *bit* so the resulting sensitivity is the cited one.



**Figure 4.3:** Positiometer

A contactless sensor, such as an Hall sensor, would have been more suitable for the application since it is more reliable, is not subject to mechanical wear and is immune to the vehicle vibrations. However, at this stage of the study, it is impossible to use due to its measure being discrete, so unsuitable for control purposes. Moreover, the prototype is made in a metallic material that could interfere with the Hall sensor measurements since they are based on a magnetic field effect.

To measure the displacement of the mechanical cable, the potentiometer is rigidly connected to the runner linked to the transmission by means of a customized 3D printed support (in blue).

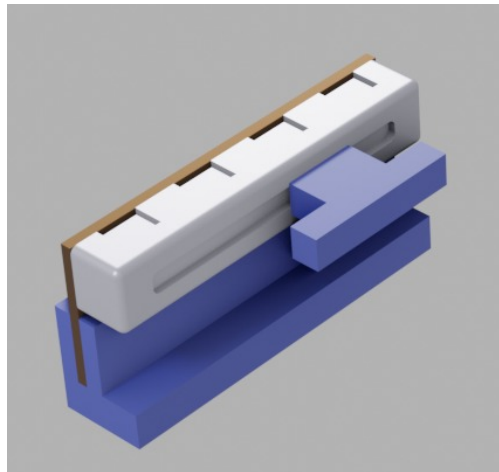


**Figure 4.4:** 3D printed potentiometer support

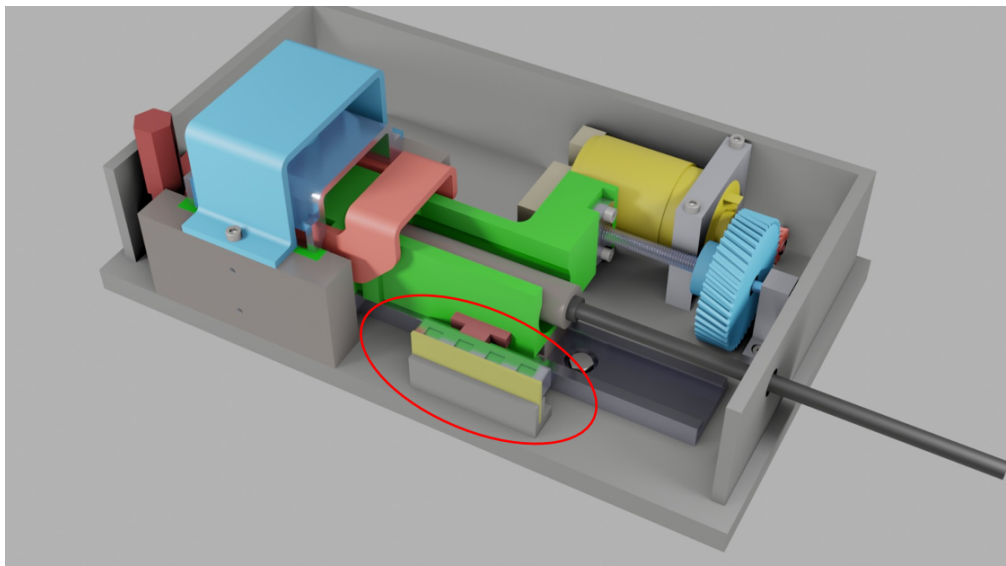


**Figure 4.5:** Potentiometer installation

## 4.2.2 Current sensor

The current sensors are devices that measure the current intensity. They can acquire the measurement through direct contact, such as an amperometer, or by means of the magnetic field, such as a current clamp.

For our application, the current sensor is not needed for control purposes, but for the model validation.

Indeed, after implementing the correct model, the values inserted in the block scheme are fundamental for the simulation accuracy. Since the DC motor datasheet is incomplete, the current sensor is fundamental to estimate certain motor parameters as it will be discussed in Chapter 5 "Model validation".

Moreover, the current sensor measure is used by the software for safety purposes. Since the current flowing into the DC motor in certain situations is greater than the DC motor rated current, if the sensor sees a higher current for too many seconds, it means a fault occurred and so the microcontroller shuts down the DC motor voltage supply.

The chosen current sensor is a sensor that exploits the Hall effect and can measure up to 20 A. The sensor sensitivity is 12 mA and the measurement error is 1.5% of the measure.

The considered sensor is the *ACS712ELC-20A* by *Allegro MicroSystems*.

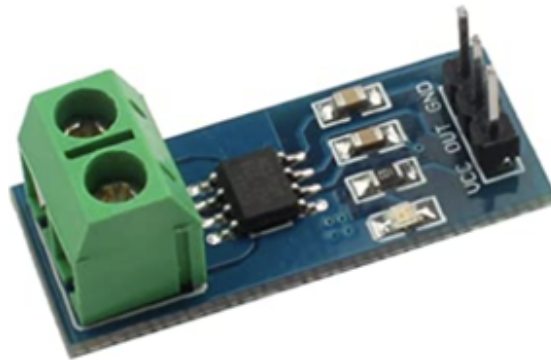


**Figure 4.6:** Current sensor

## 4.3 Motor driver

The motor driver is the component that provides to the DC motor the voltage profile computed by the control law implemented in the microcontroller firmware. Its aim is to convert the constant 12 V voltage of the power supply into a continuous variable voltage to supply the electrical motor to realise the correct movement of the mechanical cable.

It is composed by two entities:

- PWM modulation: it is the digital implemented strategy that allows the voltage profile to be continuously variable.
- H bridge: it is the hardware solution the physically supply the electrical motor

### 4.3.1 Pulse Width Modulation

The pulse width modulation, or PWM modulation, is a technique that allows to obtain a continuous variable voltage starting from a constant voltage reference. This is realised through a square wave of peak-to-peak amplitude equal to the constant voltage.

By changing the duty cycle of the square wave, the average value of the waveform changes. The duty cycle, DC, is defined as the ratio between the ON phase of the period  $T_{on}$  over the total period  $T$  of the square wave.

$$DC = \frac{T_{on}}{T}$$

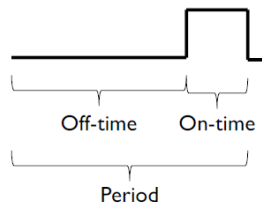


**Figure 4.7:** Square wave duty cycle

The average value of a waveform is computed as:

$$\bar{y} = \frac{1}{T} \cdot \int_0^T f(t) dt$$

For the square wave used for PWM modulation  $y_{max}$  is the constant voltage supplied while  $y_{min} = 0$ , so the formula reduces to:

$$\bar{y} = DC \cdot y_{max}$$

It can be noticed how a change in the duty cycle of the square wave leads to a change of the average voltage value.

The value of the duty cycle is computed by the control law.

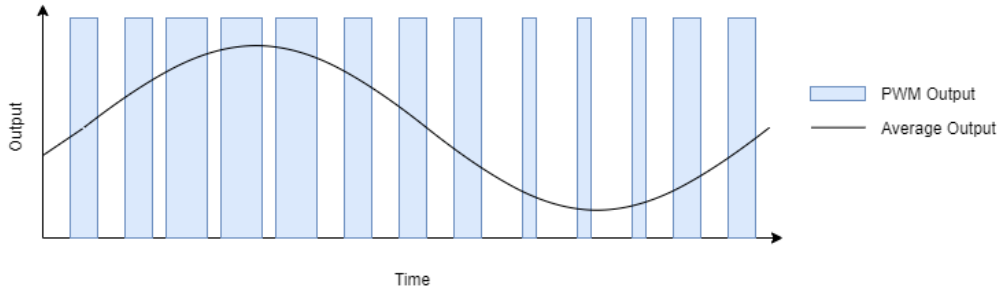


**Figure 4.8:** PWM average output voltage

The most important parameter to choose to implement the PWM modulation is the PWM frequency that is defined as the inverse of the PWM square wave period.

$$f_{PWM} = \frac{1}{T}$$

The value of this frequency is a trade off between multiple factors.

First of all, the frequency must be high enough for the electrical motor to not follow the voltage changes. In this way, even if the supplied voltage is a square wave between 12 V and 0 V, the DC motor sense only the average voltage obtained by modifying the duty cycle. In particular, since the voltage supplied is linked to the rotor angular velocity, a high PWM frequency leads to a more constant velocity due to the fact the DC motor is not able to follow the sudden changes of the PWM voltage.

A second aspect to take into account is the current behaviour. If for the supplied voltage higher the frequency, better the behaviour for the absorbed current the inverse is true. As the DC motor can be modeled essentially as a *RL circuit*, with a high PWM frequency, the current is not able to reach its steady state value resulting in a ripple behaviour over the time. Higher the frequency and lower the ripples and lower the generated torque  $T_m$  that depends on the absorbed current. A third aspect to consider is the DC motor efficiency.

As seen in the previous chapter, the DC motor has a behaviour which can be compared to a low pass filter. For this reason, the chosen PWM frequency cannot be too high in order to have a better efficiency of the system.

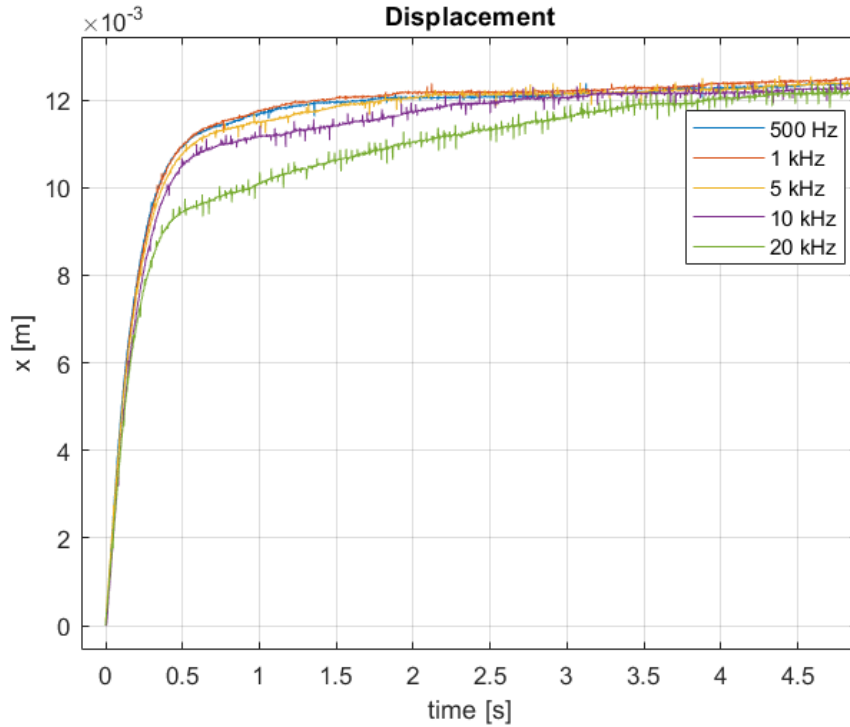


**Figure 4.9:** Mechanical cable displacement with the same voltage profile supplied to the DC motor at different PWM frequencies. Higher frequencies lead to a slowdown in the performances

The last aspect to take into account for the PWM frequency choice is the physical behaviour of the electrical motor.

The DC motor acts like a speaker amplifying the frequency at which it is supplied.

If it is supplied at low frequencies, tens of Hz, it produces vibrations, while at higher frequencies, thousands of Hz, it emits a whistle at the supplied frequency. Since the human ear can perceive the frequencies from few Hz to 20 kHz, a frequency of 20 kHz should be the best choice but for the reasons discussed above is not suitable for this DC motor.

My colleague and I, in accordance with the company, decided to set  $f_{PWM} = 10$  kHz.

### 4.3.2 PWM modelling

All the theory discussed in this section is translated into Simulink feature for the model and the simulation.

The choice of the PWM frequency affects directly the choice of the simulation step size. In discrete time simulation, the step size is the integration time step the solver uses to integrate the equations implemented by the model, so it is the time interval between two computations of the modeled quantities. The step size can be fixed or variable depending on the desired Simulink configuration. A variable step is computed at each integration time based on the modeled system dynamics while a fixed step time is constant throughout the whole simulation. To better represent the real time behaviour of the system, a discrete solver with fixed step size was used for the simulations.

Each discrete block in the model, included the control block scheme, use as sample time  $\Delta t = 1/f_{PWM}$ . The value of the solver step size need to be multiple times less than the other sample time so it is set to  $step_{size} = \frac{1}{f_{PWM}/50}$ .

The PWM behaviour is modeled as shown in Figure 4.10

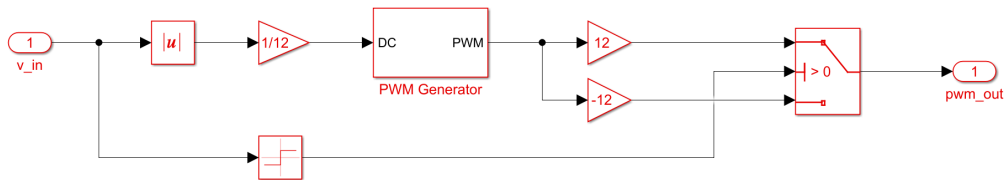


Figure 4.10: PWM block scheme

The input of this block is the voltage computed by the control law at each sample time  $T_s = 1/f_{PWM}$  while the output is the voltage supplied to the DC motor. The PWM block receives the average voltage target, compute the correlated duty cycle and generate the right square wave of amplitude 1 Vpp. The square wave is then adeguated to the system dynamics so it becomes a square wave of amplitude 12 Vpp. The sign, abs and switch block are inserted in order to be able to translate both average voltage from 0 V to 12 V and from 0 V to  $-12$  V since the DC motor rotated in both directions.

### 4.3.3 H bridge component

After understanding how the variable voltage to be supplied to the DC motor is implemented, the component that realise it must be addressed.

Since the microcontroller output voltage maximum value is 5 V while the electrical motor need to be supplied in a  $[0 - 12]$ V range and the current absorbed by the DC motor is way greater than the one circulating in the microcontrontrroller circuit, the power stage is essential to adequate the dynamic range of these quantities. Moveover, it is responsible for the realization of the rotational direction of the DC motor. The power stage chosen is the H bridge.

The H bridge is an electronic circuit that switches the polarity of the voltage applied to the load. The change in polarity of the voltage supplied to the DC motor results in the DC motor running forward and backward.

The polarity inversion is implemented by activating one on the two half bridges the circuit is composed.

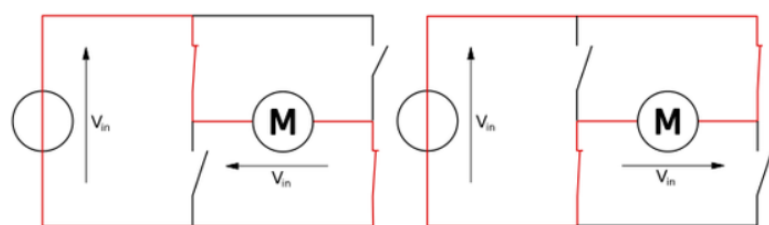
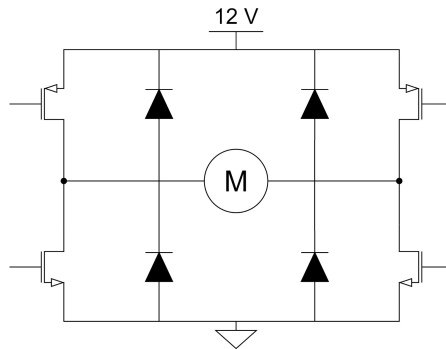


Figure 4.11: H bridge logic

The generation of the supplied voltage  $[0 - 12]V$  is obtained with the PWM technique implemented by opening and closing the switches of the half bridge enable in that time instant. The switches are implemented using transistors driven by a microcontroller signal.



**Figure 4.12:** H bridge circuit

The chosen H bridge integrated circuit is the H bridge by *Infineon Technologies* composed by the two half bridges model *BTS7960*. The component receives as input the reference voltage  $\pm 12V$ , the enable and disable signals for the half bridges, the supply voltage to run and the PWM signal for each half bridge. It was chosen because it can drive up to 40 A and it has a working voltage of 12 V. Moreover, it is automotive compliant and cost effective.

From the modelling point of view, the component behaviour is already implemented in the PWM block in Figure 4.10.

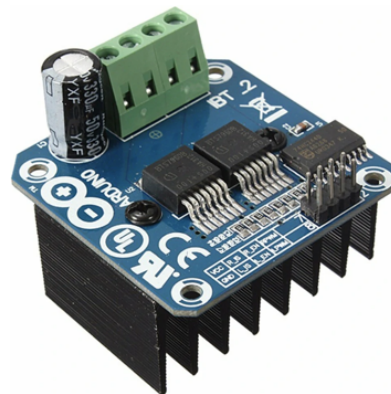


**Figure 4.13:** H bridge integrated circuit

# Chapter 5

## Model validation

The aim of a model is to represent the behaviour of the modeled system in the most possible accurate way.

To build the correct model, the block disposition and block connections are essential, but also the parameters put inside these blocks are very important and they affect the model correlation with respect to the real time behaviour. This is the reason why the validation of the model is a fundamental step in the building of the model itself.

While the block scheme implementation has been discussed in Chapter 3, the model validation will be analysed in this chapter.

The model parameters can be divided in:

- Electrical motor parameters
- Mechanical prototype-related parameters

## 5.1 DC motor validation

The most important part of the model to be validated is the electrical motor part since it is the main feature of the shifting system and its behaviour is determined by the parameters themselves.

The motor informations the manufacturer provides are the one in Table 2.1. It can be seen the datasheet is incomplete since the value of the motor inductance  $L_a$ , motor inertia  $J$  and motor friction coefficient  $\beta$  are not expressed. The motor parameters are fundamental for modelling and simulation so these data must be obtained.

To characterize a DC motor, a motor test bench is usually used. It is a measurement instrument to detect the motor parameters and other quantities in different working conditions.

Unfortunately, in the company the motor test bench is not present so my colleague and I had to choose other options using the best means available.

At first we decided to contact the manufacturer assistance service, allowing to acquire the value of the motor inertia which is a quantity impossible for us to measure.

The other mechanical quantity we cannot measure is the viscous friction coefficient  $\beta$ . Since its value is normally very small, at first it was neglected in the model but in a second moment it was set equal to  $\beta = 1 \times 10^{-6} \text{ N m s/rad}$ .

Instead, for the electrical quantities,  $R_a$  and  $L_a$  we were able to run some tests in order to estimate them.

To estimate the electrical quantities, a no load test was performed. It consisted in supply the DC motor with constant voltage in no load condition and acquired the current data through the current sensor, mentioned in the previous chapter, and the Cube MX monitor program.

From the so obtained current profile is possible to compute the electrical time constant  $\tau_a$ , defined in Equation 3.3, and the value of the motor resistance  $R_a$ .

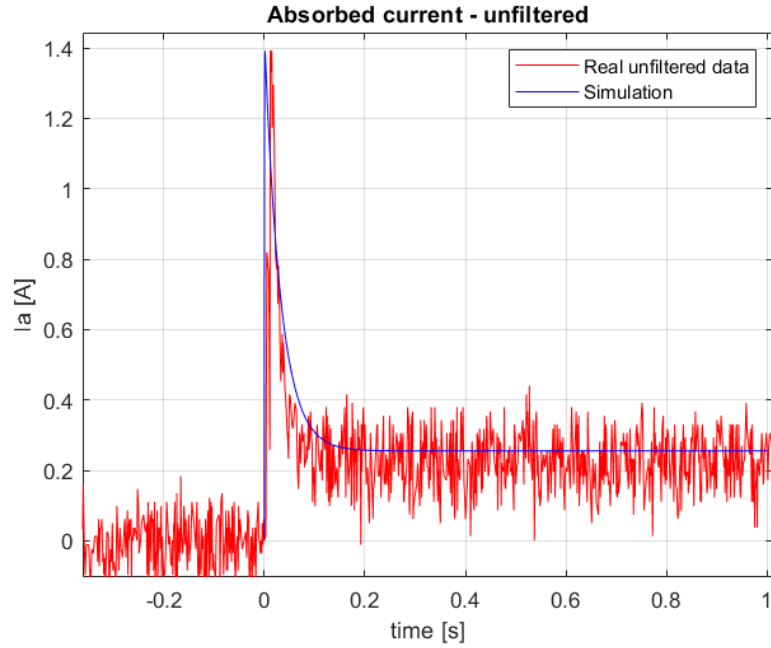


**Figure 5.1:** Unfiltered absorbed current during no load test with supplied voltage 1 V

From this profile, the value of the motor resistance  $R_a$  is computed as:

$$R_a = \frac{V}{I_{a_{peak}}} \approx 0.7 \Omega$$

The value of the motor inductance is derived from the value of the electrical time constant  $\tau_a$  known  $R_a$ .

Since the DC motor is electrically equivalent to a RL circuit, it can be said that the current reaches its steady state value ( $I_{a_{peak}}$ ) after a transient. The transient can be considered complete after  $4 - 5 \tau_a$ . For simplicity, we considered it completed after  $5\tau_a$ .

$$L_a = \tau_a \cdot R_a \approx 1.84 \times 10^{-4} \text{ H}$$

The value of the no load current, by looking at the current profile, is

$$i_0 \approx 0.25 \text{ A}$$

It is important to remark that these computations are quiet poor since obtained values vary if for example the transient is considered complete after  $4\tau_a$  or  $6\tau_a$  instead of  $5\tau_a$ .

Moreover, using a unfiltered current profile or a filtered current profile makes the parameters change even more since the current peak, and so the motor resistance  $R_a$  varies a lot, as shown in the example below. The no load current  $i_0$  remains that same as before.

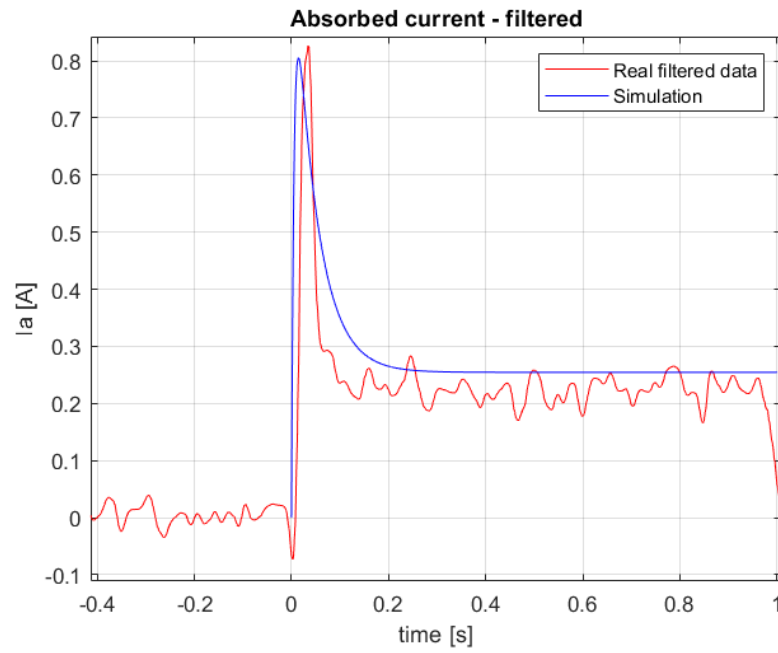


**Figure 5.2:** Filtered absorbed current during no load test with supplied voltage 1 V

The new values for the motor resistance and the inductance are:

$$R_a = 1.1 \Omega \quad L_a = 5.2 \times 10^{-3} \text{ H}$$

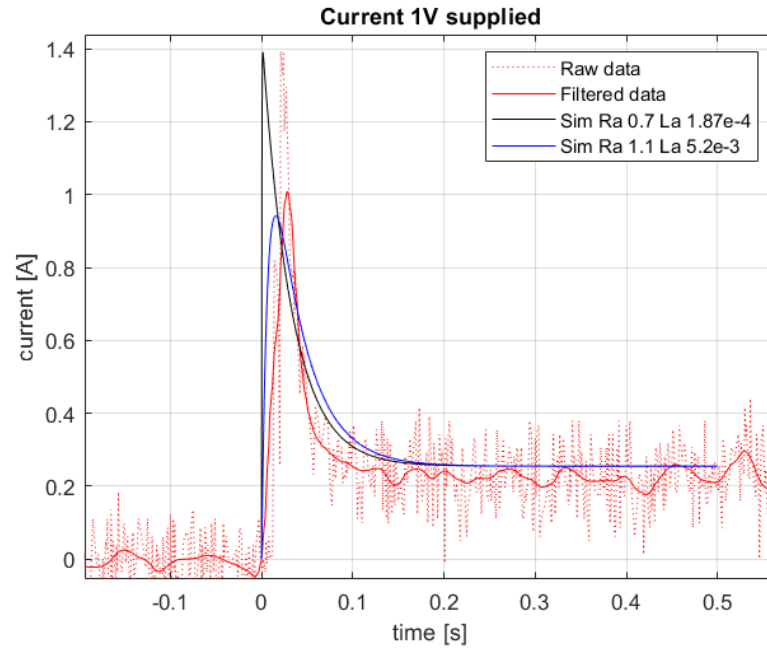


**Figure 5.3:** Absorbed current during no load test with supplied voltage 1 V - comparison between parameter set

The comparison between the two current profiles is shown in Figure 5.3. In the end, the DC motor chosen parameter set is the following:

No load current	0.25 A
Torque constant	12.6 mNm/A
Motor resistance	0.7 $\Omega$
Motor inductance	$1.84 \times 10^{-4}$ H
Motor inertia	$7.4 \times 10^{-6}$ kgm <sup>2</sup>
Viscous friction coefficient	$1 \times 10^{-6}$ Nms/rad

**Table 5.1:** Motor parameters

Since the absence of an suitable motor test bench and the tests being run in uncertainty conditions, these parameters of the motor are an estimation of the real parameters and this will produce the greater uncertainty on the model of the system.

## 5.2 Transmission and spring validation

The parameters of the mechanical components are computed by the colleague who designed the prototype.

After he chose and bought the components, he characterized them.

The resulting parameters used in the Simulink model are, for the whole transmission system, the ones shown in Table 2.2, while the spring elastic coefficient is  $k_{el} = 3.76 \times 10^3 \text{ N/m}$  and its initial compression is  $x_0 = 51.3 \times 10^{-3} \text{ m}$ .

## 5.3 Static and dynamic friction validation

An other system features to validate are the torques produced by the static and dynamic frictions. These phenomena are already implemented in the Simulink model by their block scheme, Figure 3.13, but they lack their measurements.

The static and dynamic frictions depend on the static and dynamic friction coefficients and the mass.

If the mass is a quantity easily measurable, the friction coefficients are not since they are determined by the nature of the material of the parts that are sliding, the sliding conditions, the use of lubricant media.

Normally, there are datasheets of coefficient friction but since a lubricant oil was used on the park actuator prototype, they are no longer reliable. So to measure the static and dynamic friction, our colleague used a dynamometer linked to one on the runner. The test was conducted only on one runner because they both have the same mechanical properties. In this way he derives the resistant force they generate.

To validate the measurement obtained by the colleague, my electronic colleague and I run a test evaluating the absorbed current.

The test was run with no external loads such as the presence of the mechanical cable or the gearbox resistant force, so only with the runner linked to the transmission. Since the prototype has a limited displacement stroke, the DC motor is supplied by the voltage profile computed by the controller and not with a constant voltage. The control system design will be discussed in the next chapter.

The resulting current profile is the following:

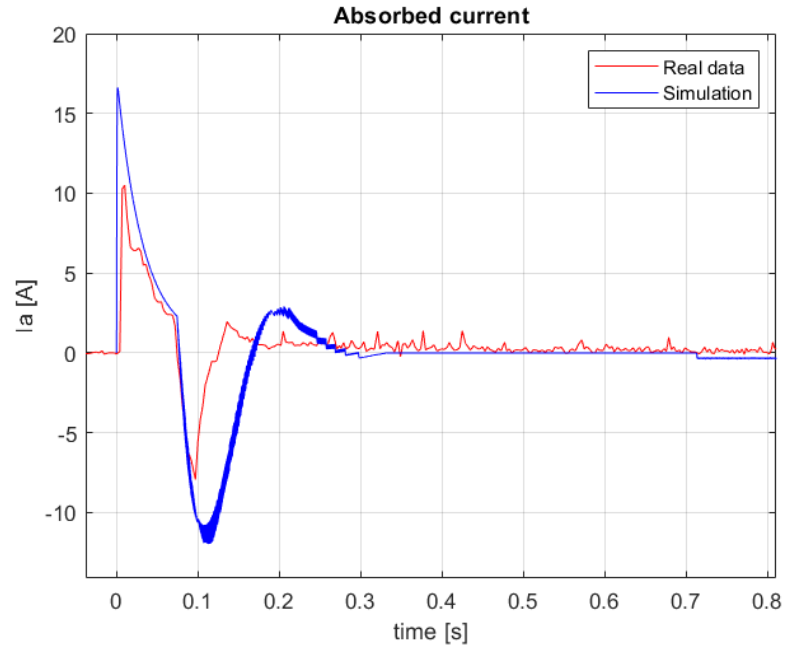


**Figure 5.4:** No load current test

To estimate the values of the static and dynamic friction torque, a trial-and-error approach was adopted. The friction parameters have been changed until the simulation was close enough to the real behaviour.

The obtained results are:

$$T_{r_{static}} = 6 \times 10^{-3} \text{ N m for the static friction}$$

$$T_{r_{dynamic}} = 2 \times 10^{-3} \text{ N m for the dynamic friction}$$

## Chapter 6

# Control design

The main purpose of this master thesis is the correct handling of the mechanical prototype. In order to do so the electrical motor has to be supplied by a voltage profile to meet the requirements on the different movements the mechanical cable has to perform. The requirements are expressed in terms of time to cover the required mechanical cable displacement, voltage limits, accuracy of the movement and loads to overcome. For this reason, a control system is fundamental to implement the correct behaviour.

A control system is a technology in which a controller compute the input to be given the system to be controlled, generally called "plant", in order to obtain a desired system behaviour.

The controller can be implemented with different techniques based on plant characteristics and on the requirements to achieve, but it always computes the input to supply to the plant (the controller output) starting from a reference signal.

## 6.1 Closed loop control system

Control systems can be divided in two categories: open loop systems and closed loop systems. An open loop system provides the input signal to the plant based only on past and present values of the reference signal, so it cannot notice external unexpected factors acting on the system such as disturbances or parameters uncertainties.

A closed loop system provides the input signal to the plant based on past and present values of the reference signal and the measured plant output, the so called "control variable". It is a more powerful architecture since it can reduce the disturbance effects acting on the system and compensate plant uncertainties.

For our application a closed loop system is chosen.

The essential elements of a closed loop control system are:

- Controller
- Actuator
- Plant
- Sensor

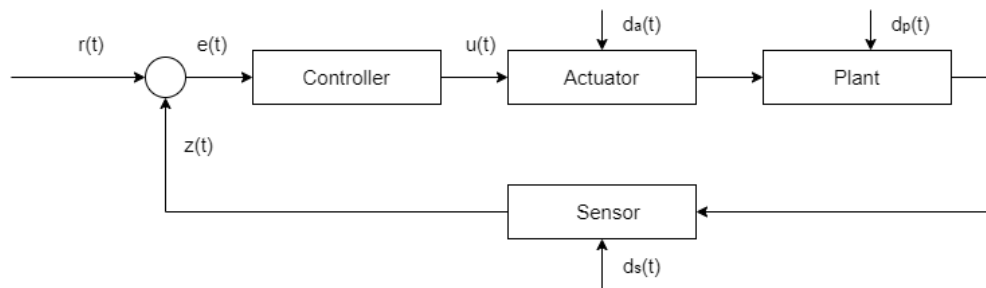


**Figure 6.1:** Closed loop system

## Controller

The controller is the core of a control system. It receives as input the error  $e(t)$  on the measured output with respect to the reference signal and compute as output  $u(t)$  the input to implement on the plant. Its aim is to make the behaviour of the plant measured output as close as possible to the reference signal.

The controller can be implement through many strategies, depending of the plant characteristics and requirements: loop shaping, PID, pole placement, H infinity norm, data driven controller, model predictive controller and many others.

For the shifting system application a PID controller is chosen.

## Actuator

The actuator is the element that physically implements the control law  $u(t)$ . It is needed to adjust the controller output dynamics to the plant dynamics. On the actuator, disturbances can act.

For the shifting system application, the actuator is the H bridge that implements the PWM modulation.

## Plant

The plant is the system to be controlled. In the control architecture, the plant is expressed as its transfer function. In our application, the transfer function is implemented through the Simulink block scheme of the system model discussed in chapter 3. On the plant, disturbances can act.

For the shifting system application, the plant is the system composed by the DC motor, the transmission and the loads acting on the DC motor. The loads due to the different situations the park actuator has to handle cannot be treated as disturbances since they are dependant on the mechanical cable displacement.

## Sensor

The sensor is the element introduced to measure the physical quantity under control, the measured plant output  $z(t)$ . On the sensor, disturbances can act.

For the shifting system application, the measured output is the linear displacement of the mechanical cable while the sensor is the potentiometer.

## 6.2 PID control strategy

The brushed permanent magnet DC motor, is a electrical machine with constant excitation flux produced by the permanent magnet, therefore the only possible regulation is the voltage regulation.

The voltage regulation consists in supplying a voltage profile to the DC motor. In our application, the controller only duty is to compute this voltage profile taking into account the movement requirements and system limitations.

The shifting system is a third order system since its transfer function has three poles.

Its response to a step reference signal is the one shown in Figure 6.2.

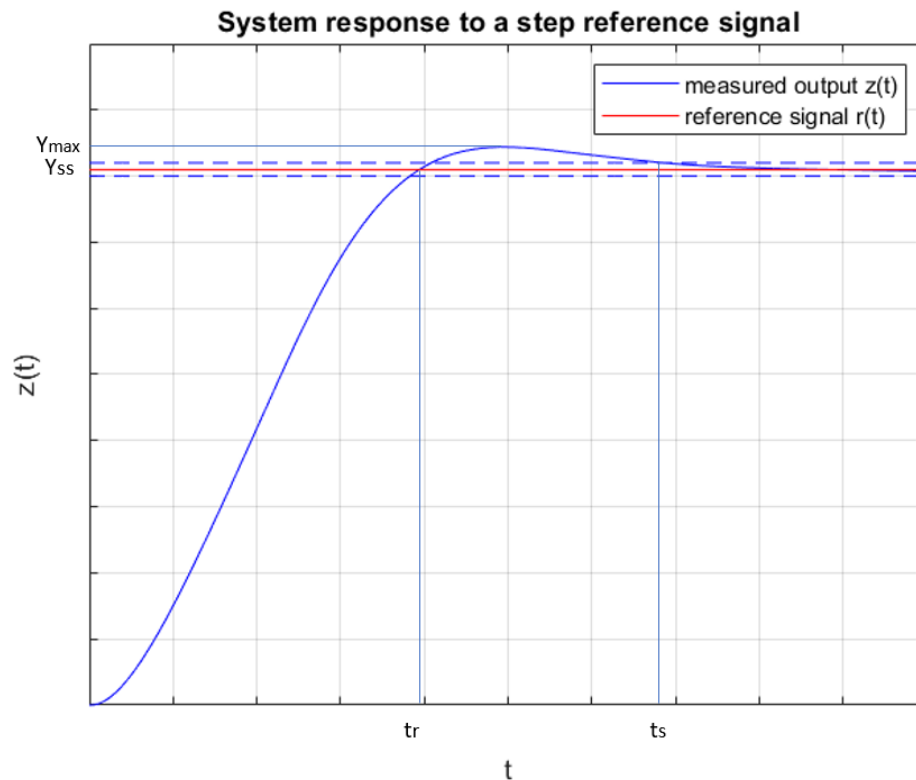


**Figure 6.2:** System response to a step reference signal

The quantities that describe the transient performance are the maximum overshoot  $\hat{s}$ , the rise time  $t_r$  and the settling time  $t_s$ .

The overshoot expresses the accuracy and is defined as:

$$\hat{s} = \frac{y_{max} - y_{ss}}{y_{ss}}$$

where  $y_{max}$  is the maximum value the measured output  $z(t)$  reaches and  $y_{ss}$  is its steady state value at the end of the transient.

The rise time is the first moment the measured output  $z(t)$  reaches its steady state value and it expresses the trigger off quickness of the system.

The settling time is the time the system needs to reach and stay in a uncertainty range of error around the steady state value and it expresses the extinction quickness of the transient.

The chosen control technology for the application is the PID technique which is a simple procedure that can be summarize into the choice of three parameters to influence the system behaviour.

In continuous time, the PID control law is the following:

$$u(t) = K_p \cdot e(t) + K_i \int_0^T e(t) dt + K_d \cdot \frac{de(t)}{dt} \quad (6.1)$$

where  $e(t)$  is the error computed as

$$e(t) = r(t) - z(t)$$

where  $r(t)$  is the reference signal and  $z(t)$  the measured output signal.

The control law is composed by three contributions, each of them weighted by a coefficient:

- Proportional contribution with coefficient  $K_p$ : it implements a proportional action. It reduces the rise time and the steady state error, it increases the overshoot.
- Integrative contribution with coefficient  $K_i$ : it implements an integral action. It eliminates the steady state error and increases the overshoot.

- Derivative contribution with coefficient  $K_d$ : it implements a derivative action. It increases the phase margin and the command activity, it reduces the overshoot.

Depending of the contribution needed for the application, it is possible to have all combination of controllers: P controller, PI controller, PID controller, PD controller and so on.

## 6.3 PI modelling

For our aim, a PI controller will be implemented. In order to tune the three parameters of the PI controller, the simulation is essential, so the whole control system has to be implemented in Simulink.

The plant block is already done while the controller has to be modelled and the same approach used for the plant will be adopt.

The actuator, the H bridge, as said before does not need to be model since it does not introduce in the system any gain or delay or other effects to be considered.

The same goes for the sensor.

As done for the shifting system, to model the PID controller the starting point is the translation of its continuous time function, Equation 6.1 into its transfer function in *Laplace* domain obtaining:

$$\frac{U(s)}{E(s)} = K_p + \frac{K_i}{s} + s \cdot K_d \quad (6.2)$$

This equation is then converted into the discrete time *z transform* domain and implemented in the block scheme: Figure 6.3, Figure 6.4, Figure 6.5

In the PI block scheme, a saturation block is added because the control law must be in the range between  $-12\text{ V}$  and  $12\text{ V}$ .

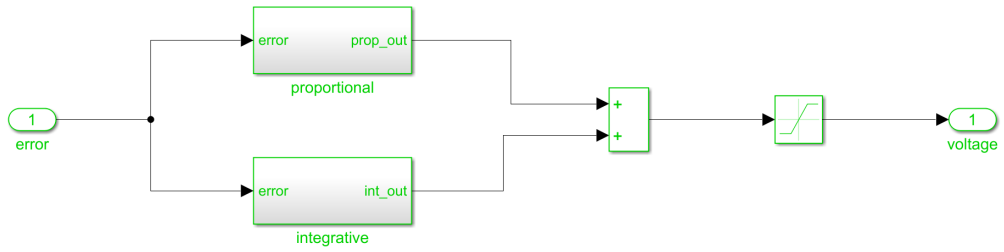


**Figure 6.3:** PI block scheme

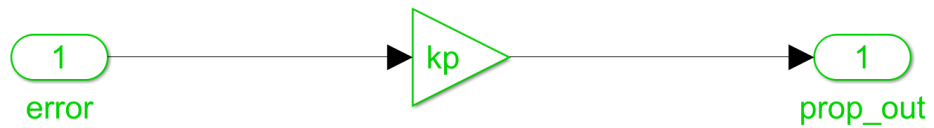


**Figure 6.4:** Proportional contribution block scheme

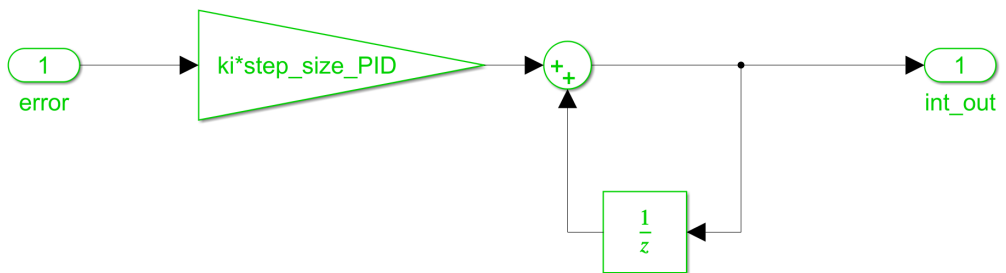


**Figure 6.5:** Integrative contribution block scheme

## 6.4 PI tuning

Once the model is implemented, the PI controller can be tune to satisfy the functional requirements.

For each operation condition, the tuning has been performed with a trial and error procedure using the simulations of the implemented closed loop control system. This is the reason why the system model has different load blocks implemented separately. By connecting the right block in the model, that specific handling situation can be study and used to tune the PI controller for that specific movement. For every movement, the constant position target and the transient characteristics are defined (overshoot, settling time, rise time).

The different conditions the controller has to implement are:

- No load condition: only the DC motor and the transmission and their friction loads are present in the model.
- Spring loading: the spring load and the runners friction are considered. In this case the settling time is not important since when the bridge of the retaining system is in contact with the electromagnet the system is keep place with no possibility of motion. Moreover this is the most dangerous handling since to compress the spring the DC motor absorbs a current higher than the rated current. If this kind of absorption last over time it can damage the DC motor, so it is important this handling is fast enough to remain in safety conditions.
- P - not P movement: the P - not P load is considered. The position target and the settling and rise time depend on the gearbox specifications.

The results of the tuning are shown in the next chapter.

After finding the correct set of parameters of the PI controller, the controller itself is implemented in the microcontroller firmware by my colleague, since the closed loop controller works in real time during the handling.

In the firmware, a "stop condition" is implement to turn off the DC motor after a certain amount of time the mechanical cable position is inside the uncertainty error range around the measured output steady state value.

# Chapter 7

## Testing

The testing phase is the last phase in the project work flow. It was carry out in the company laboratory and consisted in testing multiple times all the required park actuator handlings.

The tests allow us to understand if our work was suitable for the implementation and, if necessary, make some adjustments.

Summarizing, in the all considered scenarios, the aim is to test:

- The mechanical prototype adequacy and robustness
- The robustness of the Simulink model and the suitability of the control system and the correlation between physical system behaviour and simulated behaviour
- The correctness of the hardware and firmware to implement the correct action on the physical prototype

It is important to highlight again that the goal of this work is to study and comprehend how this kind of object can be design in model based approach, rather than having a perfectly functioning actuator. For this reason, also tests like the no load condition, which is a functional scenario that is no taken into account, are run.

Moreover, during the testing of the movement P - not P on the test gearbox an error in the physical set up of the test was made. This error changes the load profile.

Since the purpose of this thesis is also to verify the correlation between the physical system and its modelling, in the block scheme the load block corresponding to this scenario was modified to recreate what happened during the test.

## 7.1 No load condition test

The first test performed is the no load test in which only the runners without the mechanical cable are handled.

In particular, the goals of this test are:

- Estimation of static and dynamic friction
- Test the robustness and correct behaviour of the mechanical prototype

The first goal is the estimation of the static and dynamic friction; how the test, in particular the current profile, is exploited is analyzed in the Chapter 5 "Model validation".

The second goal is to check the correct functioning of the mechanical prototype designed previously by the other colleague.

To assess this aspect, choosing the corresponding PI tuning, the handling was performed hundred on times in sequence.

It resulted in the addition of thrust bearings of the screw-nut transmission system to avoid wear of the screw support.

The data from the test are acquired by the sensors and compared with respect to the simulated data as shown in Figure 7.1, Figure 7.2, Figure 7.3.

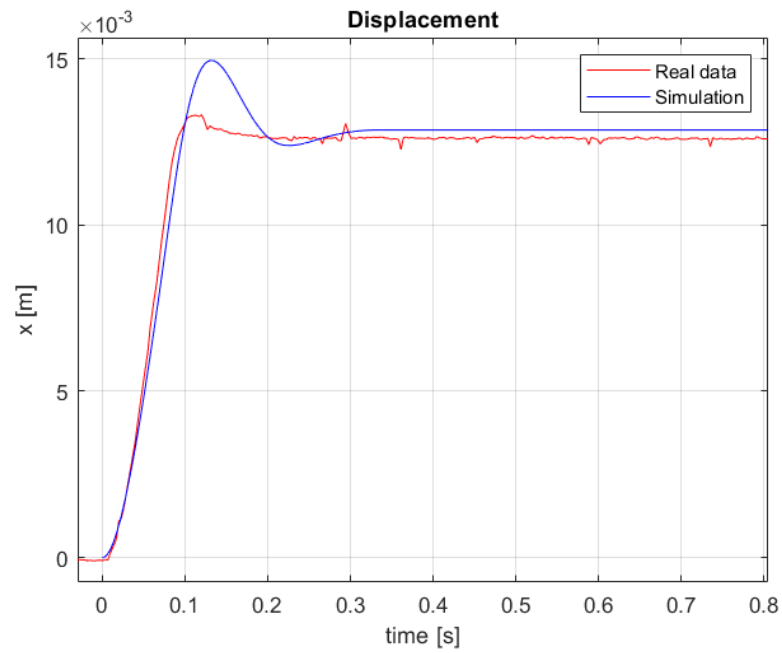


Figure 7.1: No load condition test - displacement

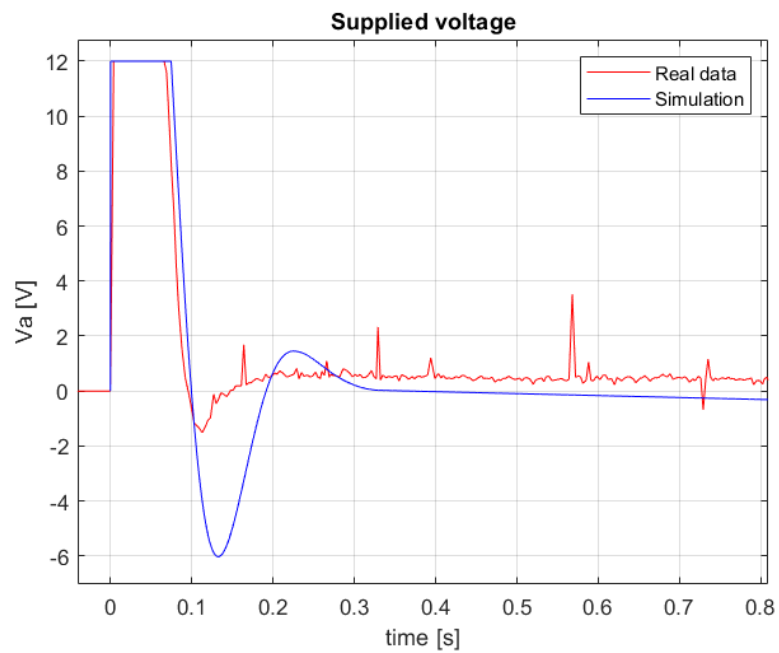
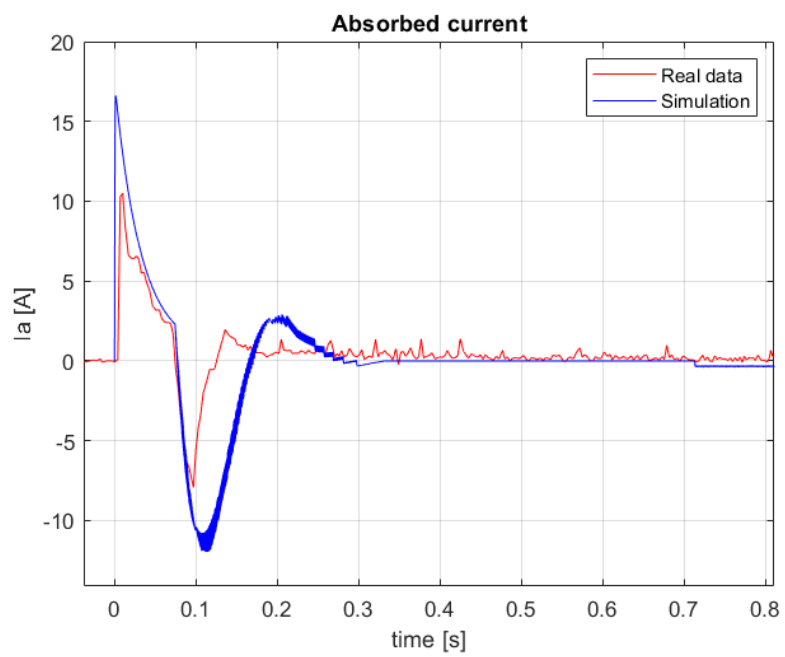


Figure 7.2: No load condition test - supplied voltage



**Figure 7.3:** No load condition test - absorbed current

## 7.2 Spring loading test

The spring loading test is, together with the no load test, to characterized and, if necessary, adapt the mechanical prototype.

The test is run by loading the spring verifying the correct functioning of the electromagnet. The electromagnet is not a driven component, it is simply connected to the 12 V voltage supply, so to load the spring and active the retaining system is important to check that, once the position target, and so the spring compression, is reached the bridge of the retaining system is attracted by the electromagnet so it is possible to turn off the DC motor. If this condition is not verify, the control system is still acting on the electrical motor resulting in it absorbing a current higher than the rated one which can lead to motor damages. This test leads to the mechanical adjustment of a swing bridge to let the electromagnet attract the bridge even if they are not aligned.

The test for the emergency function was run in this moment as cycle of loading and discharging the spring, but since it is a purely mechanical condition we just evaluate the prototype correct behaviour.

The data from the test are acquired by the sensors and compared with respect to the simulated data as shown in Figure 7.4, Figure 7.5, Figure 7.6.

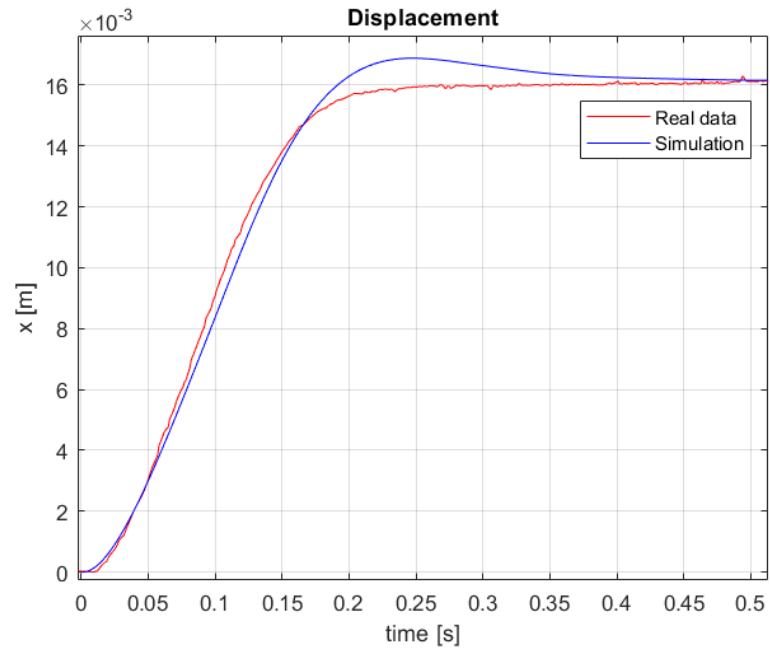


Figure 7.4: Spring loading test - displacement

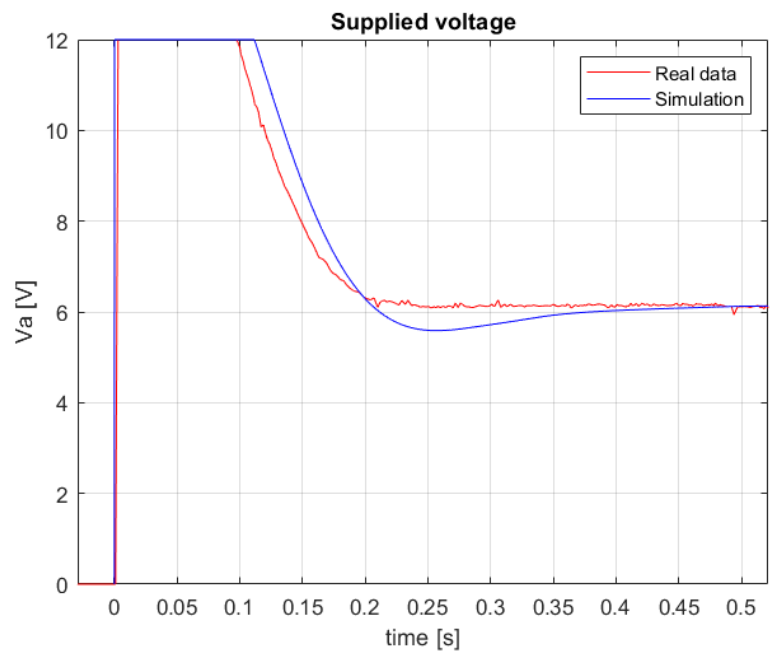
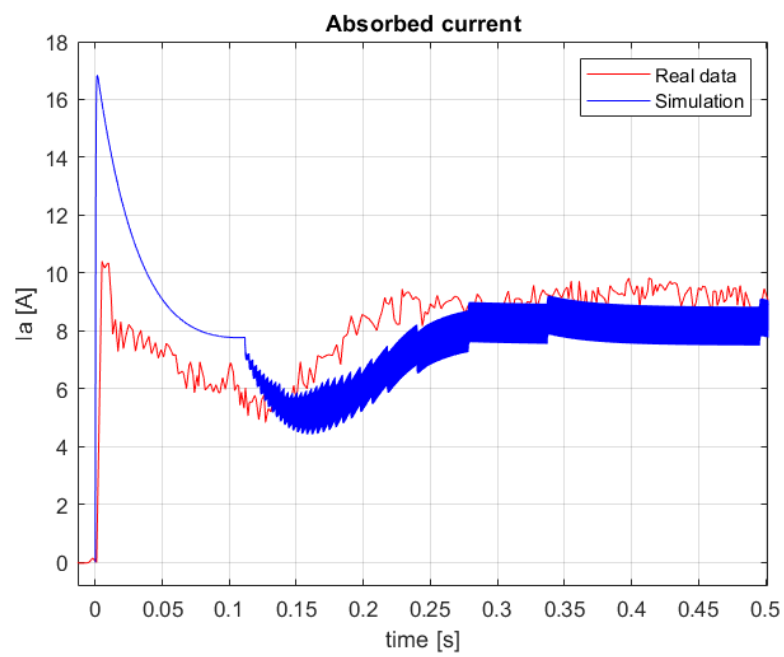


Figure 7.5: Spring loading test - supplied voltage



**Figure 7.6:** Spring loading test - absorbed current

### 7.3 Disengaging P mode test

The last test is the one acting of the test gearbox. It is performed by connecting the shifting system mechanical cable to the selector lever of the gearbox.

The aim of this test is to assess the behaviour of the complete shifting system prototype in the real working condition of engaging/disengaging P mode.

The test was run in not ideal conditions since the test gearbox presents different P - not P displacement so we have to exploit the R - N stroke for the test. Also we had a short time range to perform it and the set up was not the correct one and so an adjustment was made in the simulation to represent the real testing conditions. However, the results show the correlation between real and simulating data, achieving our goal.

In this case, the data are acquired from two tests, *Test 1* and *Test 2*. The data from the tests are compared with respect to the simulated data as shown in Figure 7.7, Figure 7.8, Figure 7.9.

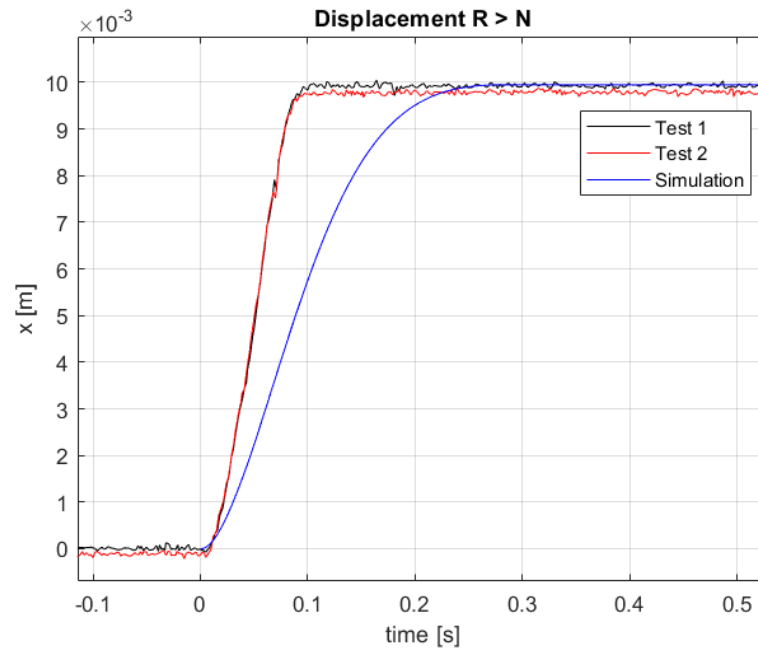


Figure 7.7: Disengaging P mode test - displacement

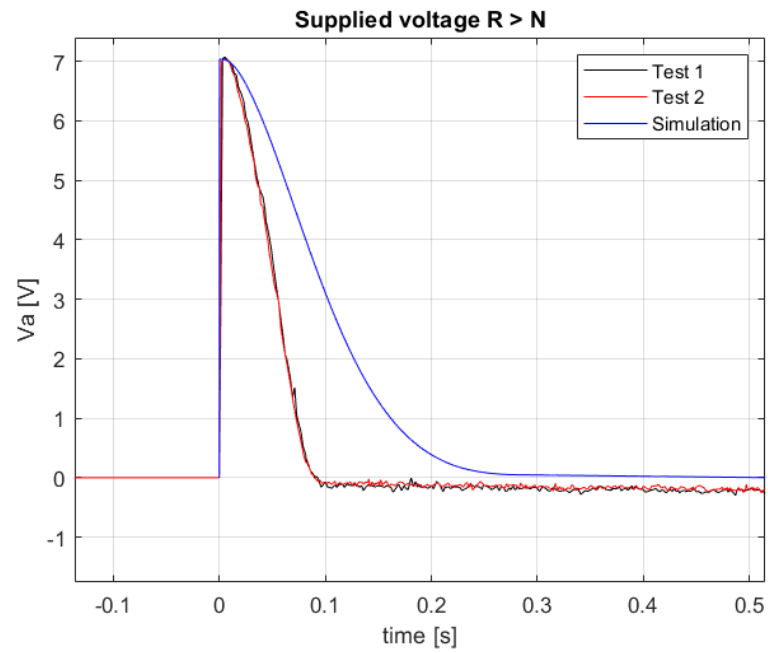


Figure 7.8: Disengaging P mode test - supplied voltage

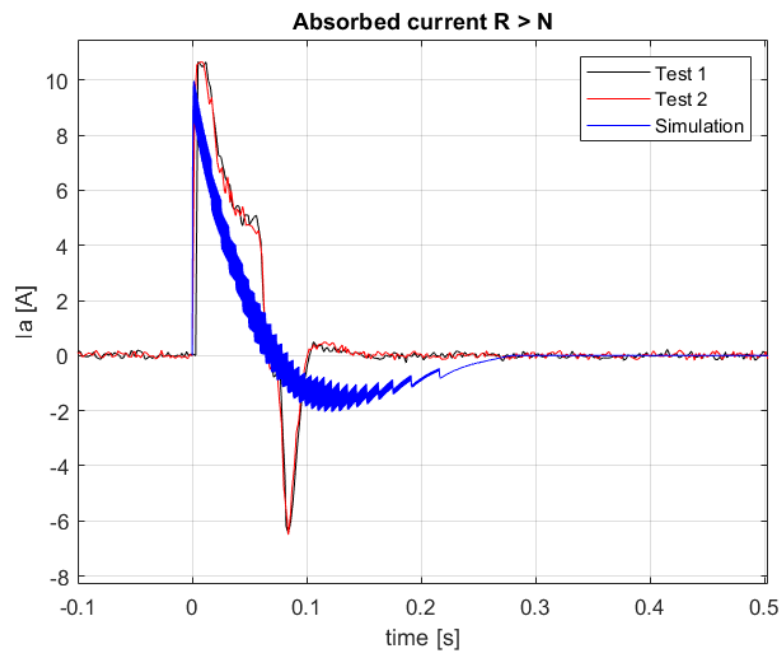


Figure 7.9: Disengaging P mode test - absorbed current

## Chapter 8

# Conclusions

Starting from the customer functional requirements and previous company studies, a working prototype of the park actuator is realised, demonstrating the validity of the model based approach.

For the part of the project I deal with, using the already existing mechanical prototype, a Simulink model is correctly built as shown in the behaviour of the tested quantities profiles being comparable with the simulated ones.

Even if the model is not perfect, it is a mathematical representation and so it will never act exactly like the system itself and it was built with the available means which were not always ideal, it is accurate enough to implement a closed loop control system that achieves the wanted handling of the mechanical cable respecting the requirements that have been given to us.

Future developments of this project are meant to realise an industrial component.

The mechanical system will be made less rigid in order to better deal with vibrations caused by the handling and the imperfect alignment of the elements, made in cheaper and lighter material that will not cause interference with a contactless position sensor replacing the potentiometer.

The model will be improved both in the block structures and in the validation of the parameters, possibly using a motor test bench to determine with higher accuracy the electrical motor parameters.

Also they will be implemented further driving modes besides P and not P, both in

the model and so in the controller tuning, in the mechanical part by extending the mechanical cable stroke and in the firmware.

The hardware part will be replaced with automotive compliant components and the firmware will be optimised.

Also all the features related to the functional safety, such as watch dogs and other more, will be implemented.

Moreover the CAN communication protocol to receive the signal from the human driver will be implemented.

# Bibliography

- [1] Gene F Franklin, J David Powell, Abbas Emami-Naeini, and J David Powell. *Feedback control of dynamic systems*. Vol. 4. Prentice hall Upper Saddle River, NJ, 2002.
- [2] Jan A Melkebeek. *Electrical machines and drives: fundamentals and advanced modelling*. Springer, 2018.
- [3] Giovanni Legnani, Riccardo Adamini, Monica Tiboni, and Diego Tosi. *Mecanica degli Azionamenti. Azionamenti Elettrici: Principi di funzionamento, accoppiamento con il carico, scelta del gruppo motore-riduttore, leggi di moto, controllo*. Società Editrice Esculapio, 2016.
- [4] *Sila Group*. <https://www.grupposila.com/>.
- [5] *STM32F411RE webpage*. <https://www.st.com/en/evaluation-tools/nucleo-f411re.html>.
- [6] *Discovery PID control*. <https://it.mathworks.com/discovery/pid-control.html>.
- [7] *Using Simulink in modeling*. [https://it.mathworks.com/help/simulink/mdl\\_gd/maab/using-simulink-and-stateflow-in-modeling.html](https://it.mathworks.com/help/simulink/mdl_gd/maab/using-simulink-and-stateflow-in-modeling.html).
- [8] *MAB Modeling Guidelines*. <https://it.mathworks.com/help/simulink/mab-modeling-guidelines.html>.